AD-A067 927 MCDONNELL DOUGLAS ASTRONAUTICS CO HUNTINGTON BEACH CALIF F/G 20/4
OPTIMUM TAIL FAIRINGS FOR BODIES OF REVOLUTION.(U)
MAR 79 A M SMITH, T R STOKES, R S LEE N00014-77-C-0672
UNCLASSIFIED MDC-G7823 NL

| OF |
ADA
067927

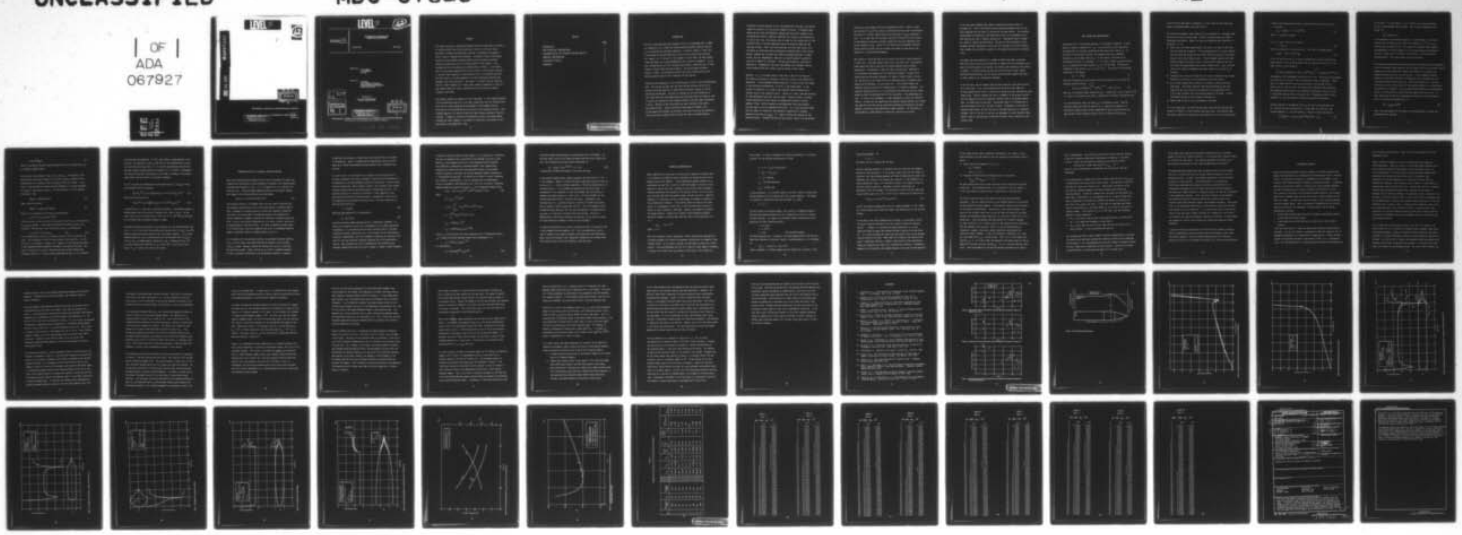

END
DATE
FILMED
6-79
DDC

LEVEL II

12

B.S.

AD A067927

DDC FILE COPY

DDC
RECEIVED
APR 26 1979
D

MCDONNELL DOUGLAS ASTRONAUTICS COMPANY

DISTRIBUTION STATEMENT A
Approved for public release;
Distribution Unlimited

MCDONNELL DOUGLAS CORPORATION

79 04 25 008

LEVEL II

12

MCDONNELL DOUGLAS CORPORATION

OPTIMUM TAIL FAIRINGS FOR BODIES OF REVOLUTION

MARCH 1979

MDC G7823

PREPARED BY:

A. M. O. SMITH
T. R. STOKES, JR.
R. S. LEE

APPROVED BY:

J. XERIKOS
CHIEF TECHNOLOGY ENGINEER
AERODYNAMICS & HYDRODYNAMICS
VEHICLE, ENERGY & BIOTECHNOLOGY
ENGINEERING DIVISION

PREPARED FOR:

NAVAL SEA SYSTEMS COMMAND
CONTRACT N00014-77-C-0672

MCDONNELL DOUGLAS ASTRONAUTICS COMPANY-HUNTINGTON BEACH
5301 Bolsa Avenue Huntington Beach, California 92647 (714) 896-3311

ABSTRACT

This report describes a computerized method that will design tails for bodies of revolution that satisfy the Stratford criterion for zero wall shear. Stratford's original two-dimensional solution is extended to axisymmetric flow in order to implement the procedure. The method involves simultaneous solution of the extended Stratford equation and the necessary boundary conditions through the use of an inverse potential flow program. Tails designed with this procedure can be categorized as follows: 1) The entire tail is at incipient separation (no skin friction); 2) The pressure recovery is the most rapid possible; 3) The resultant tail is the shortest possible. The final result is a unique geometry for given freestream conditions and boundary layer transition point. By unique, it is meant that any deviation from the "ideal" geometry will either cause extensive separation or the tail must become longer and, hence, contribute to skin friction and reduced volumetric efficiency.

The computer program can operate in one of two modes: 1) The forebody geometry can be maintained (except for a very small region near the tail juncture) with only the tail shape determined by the method; 2) The forebody velocity distribution can be maintained up to the point of the pressure recovery. The forebody geometry will then be altered for some distance upstream of the tail juncture. A number of solutions are presented for both of the above modes. Although the report emphasis is on bodies of revolution, the concept is also applicable to two-dimensional flows.

CONTENTS

INTRODUCTION

The tail of any body that moves through a fluid is an appendage that is added to "streamline" or to reduce the drag by permitting better pressure recovery. It is not necessarily desirable otherwise. If overall length is fixed, part of the volume of the main body must be sacrificed to provide the necessary tail length. Or, if the tail is just added to a basic body, the body becomes longer and hence is at some disadvantage from a logistics standpoint. In any case, shortening the tail will increase the prismatic coefficient and, if done properly, should reduce the drag slightly. The gains become relatively greater if there is considerable laminar flow on the forebody because tail designs properly made for this situation are even shorter.

Stratford flows (Reference 1) are limiting types of flows in the two-dimensional case. By limiting, we mean that the flows provide the most rapid rise in pressure along the body that is theoretically possible, subject to certain simplifying assumptions. One fact of interest and of great importance is that these flows have been demonstrated and have been found to be docile, that is they do not separate at the slightest deviation from the ideal (References 2 and 3). Because of this verification by test, Stratford flows should be studied further. Inverse solutions by more powerful methods, such as the Cebeci-Smith method, are possible, but they do not have the backing of direct test data to support their accuracy and their off-design behavior.

Stratford's solution applies only for two-dimensional flows and a way need be sought for applying it to the axially symmetric problem. In boundary-layer theory the Levy-Lees transformation reduces both the axially symmetric and two-dimensional flows to identical equations (for instance, see Reference 4). In view of this fact, the original plan of study for this project was to find Stratford flows in the two-dimensional plane and transform them into the Levy-Lees ξ-plane. Then, since this plane was valid for both cases, tails for bodies of revolution would be designed by examining them in the ξ-plane. However, between the time when this study was proposed and when it became active, work was independently under way to extend Stratford's separation criterion to bodies of revolution. The work was successful, resulting in Reference 5. Subsequently, ways were seen whereby this extended criterion could be applied with more finesse than by working in the ξ-plane.

Moreover, if r_0 is the body radius at the start of the tail fairing and r the radius at any point on the body, a ratio r_0/r arises in the formula for separation. In the extended Stratford analysis, it occurs to the first power. In the Levy-Lees transformation, it occurs in the second power. If the analysis of Reference 5 is correct, the Stratford relation should have a constant value at the separation point. Figures 1a, b and c show the value for all the experimental data that could be found. Figure 1a shows a straightforward application of the original two-dimensional formula to axially symmetric flows. Earlier studies of two-dimensional flows had yielded a constant equal to 0.5 as indicated by the arrow. It is seen from this figure that for bodies of revolution, the constant at separation is variable, appearing to be zero at $r_{sep}/r_0 = 0$. Figure 1b plots the constant for the extended formula. Although the data has much scatter, there is no discernible

variation of the constant from its two-dimensional value. Figure 1c shows the variation if $(r_o/r)^2$ was used as indicated by the Levy-Lees transformation. Now there is a distinct upward trend of the constant as r_{sep}/r_o approaches zero. It is clear that, of the three, the data of Figure 1b are the nearest to representing a universal constant suitable for both two-dimensional and axially symmetric flows. Hence, for the reason that the extended Stratford method could be applied with more finesse and seemed to agree better with experiment, it was the method adopted.

Most bodies of revolution that are of practical use have a running propeller at their rear. One might suspect that, with a very short tail, the propeller might modify the flow so much that the present designs might be unduly conservative. Fortunately, it does not seem to be the case. Reference 6 is an extensive investigation of the interaction problem. On page 43 the authors make the following statement, "As shown in (their) Figures 12a and 12b, the suction of the propeller did not change the point of boundary-layer separation on Afterbody 3 (a very blunt tail). The distance between the propeller plane and the point of separation was 1.3 propeller diameters. The propeller induced velocity at 1.3 D_p upstream of the propeller was not strong enough to alter the characteristics of the separation." The parentheses are ours. In view of this statement, it seems reasonable to ignore the propeller effects. A blunt tail may complicate the propeller design problem, but in these days when the flow field can be calculated accurately and propellers are wake adapted, no particular body modification seems necessary. So the bodies to be presented are simple bodies of revolution, faired out to a point.

In the most exact boundary-layer theory, transverse curvature effect is accounted for. This is the effect occurring when the boundary-layer is very thick compared with the radius of the body at the same station. The Stratford method makes no accounting of the effect and so may be in considerable error when applied very near a slender, pointed tail. Experimental work is needed as a guide to improve this deficiency. The work of Patel (Reference 7) and Nakayama and Patel (Reference 8) deal with this problem but trying to combine their methods with Stratford's approach is far beyond the scope of the present study.

The shapes and some properties of a number of bodies have been calculated. Many basic kinds of pressure distributions or shapes could be considered, but in order to avoid excessive calculations, the studies were confined to two classes of bodies: (1) bodies having constant velocity over much of their length - modified Reichardt bodies, and (2) bodies having constant diameter over much of their length as for conventional torpedoes.

As will be seen, the tail shapes that have been found are quite short and are of a reflex type. D. M. Nelson (Reference 9) did work on this same tail fairing problem and arrived at a similar tail design which was confirmed by wind-tunnel tests. Nelson's approach was not as systematic as the present one and also his method did not truly represent limiting flows as the present method does. He worked out only one case. The present report is a presentation of the true shortest tails for a variety of cases. Furthermore, in the case of Reichardt type bodies, the tail and rest of the body shape are all integrated together, that is, the tail is not just an appendage on a basic Reichardt body. Nelson's work is the only work of which we are aware, that is parallel to the present study.

SOME THEORETICAL CONSIDERATIONS

The general kind of flow being analyzed is illustrated in Figure 2. A flow begins to retard at some point $s = s_o$. In the vicinity of this same point the body begins to converge significantly from some initial radius r_o. At the start of the pressure recovery, the boundary layer has a momentum thickness θ_o and an edge velocity u_o. In the analysis the notion of an equivalent flat plate is introduced. It is of such a length, s_o, with velocity, u_o, as to generate the same thickness, θ_o, as the real body. Pressures are referenced to the velocity, u_o, at s_o, not to u_∞. In particular, the pressure coefficient is defined as:

$$\bar{C}_p = 1 - u^2/u_o^2 \qquad (1)$$

With this introduction to the notation and flow situation, we can write the extended Stratford formula. It is:

$$\bar{C}_p \left[s\,(r_o/r)(d\bar{C}_p/ds)\right]^{1/2} (10^{-6}R_o)^{-1/10} = 0.50,\ \bar{C}_p \leq 4/7 \qquad (2)$$

where R_o is a Reynolds number defined as $u_o s/\nu$. Separation is said to occur if the L.H. side of (2) exceeds 0.50, which is the empirical constant discussed earlier.

In a two-dimensional flow, the ratio r_o/r is replaced by unity. Then for incipient separation along the body aft of s_o, equation (2) amounts to a differential equation which can be integrated for $\bar{C}_p(s)$ once and for all to show the most rapid allowable pressure rise as a function of R_o and s_o.

In fact this has been done in references 1, 2 and 3 and the flows have been tested as mentioned before, with good results.

For the axially symmetric case, however, $\bar{C}_p$ is a function of r, the body shape. Since we do not know the body shape a priori, we cannot obtain any simple integrated relationship. Rather, an iterative method has been found that is successful. It is:

a) Start with a full body shape having a tail that is as close to the final one as we know how to specify. If the forward portion is to have constant velocity, then the forward portion should initially be that of a Reichardt body of the correct fineness ratio. A direct Neumann solution will then indicate closely the correct level of velocity ratio needed to get the final body with approximately the correct fineness ratio. Also, with the initial tail shape, the Neumann calculation supplies an initial $\bar{C}_p$ (s) relation.

b) Introduce the current tail shape into (2) so that integration may proceed. Now both C_p (s) and $\bar{C}_p$ (s) are available for the tail portion.

c) By an inverse method such as James's or Bristow's, calculate the new body shape. The forward pressures have been established by the basic body while the rear pressures are supplied by the integration of (2). A tail shape different from the starting shape will be found. In fact, the forward portion will be slightly different also.

d) Repeat steps b) and c) until convergence is obtained.

It is well known that, for semi-infinite cones, the velocity along the cone varies as s^m where s is slant distance from the vertex. Then assuming that this power relation still applies for very short tails (it is not certain that

it does), and translating the origin so that the vertex of the tail is at s = a we have:

$$\bar{C}_p = 1-u^2/u_o^2 = 1 - c^2\ (s-a)^{2m}/u_o^2 \tag{3}$$

where c is a general constant.

Also, for cones with b as a constant:

$$r = -b(s-a) \tag{4}$$

We wish to evaluate (2) at the very tail. Then from (3) compute $d\bar{C}_p/ds$.

$$d\bar{C}_p/ds = -2mc^2\ (s-a)^{2m-1}/u_o^2 \tag{5}$$

In (2), at the very tail, $\bar{C}_p$ is unity, assuming that the semi-infinite cone theory applies. Thus we may evaluate only the square root term of (2). We have, since R_o is not singular,

$$\left[-a\ [b(s_o-a)]/[b(s-a)]\ \ 2mc^2\ (s-a)^{2m-1}/u_o^2\right]^{1/2} = \text{constant}\ (s-a)^{m-1} \tag{6}$$

The quantity in (6) approaches infinity at s=a if m<1. The value m=1 corresponds to a blunt tail, so any tail that is pointed will have a singularity. Therefore it is seen that (2) is not exactly correct at the pointed end of a conical tail in inviscid flow. Of course, due to boundary layer thickening and subsequent modifications to the pressure distribution at the tail, such a singularity does not exist in any real flow. Alternately, the tail could terminate in a cusp and analytic singularities would be eliminated.

The next question is the behavior of $\bar{C}_p$ at the start of the pressure rise. It is easily found by integrating (2). Assume that the origin of a new distance measure, s', is at the point s_o. Then (2) can be re-written as

$$\bar{C}_p^{\ 2}\ d\bar{C}_p/ds' = 0.25\ (r/r_o)(10^{-6}\ R_o)^{1/5}/(s' + s_o) \tag{7}$$

In (7) near s' = 0, the term $(s' + s_o)$ is finite, so is R_o and the term (r/r_o) is approximately equal to unity. Thus, we have, remembering that $\overline{C}_p(s_0) = 0$,

$$\overline{C}_p^{\,3} = \text{constant } (s')$$

at the beginning of the pressure recovery. In other words, if a limiting pressure rise is sought, $\overline{C}_p$ will begin to increase as $(s')^{1/3}$ at s_0, an infinite rate of pressure rise. This result for Stratford flows, whether two-dimensional or axially symmetric, is surprising and quite interesting. It tells us that, even if a pressure rise is small, it can be initially extremely rapid. Tests seem to bear out this conclusion.

The Levy-Lees transformation transforms both the two-dimensional and axisymmetric form of the boundary layer equation into one common form in the so-called ξ-plane. Probably the simplest method of studying the problem is to transform the extended Stratford equation into the ξ-plane. If the extended Stratford equation is consistent with what is indicated by the ξ transformation, all r variation effects should cancel out. Start with equation (2). The term involving R_o varies so slowly that for the present purposes it is satisfactory to regard it as a constant. Also, $\overline{C}_p$ remains unaffected by the transformation. Hence, it is sufficient to consider only the square root term in (2). In fact, when using (2) the only transformation involved is for the distance s. For it, the Levy-Lees transformation is

$$d\xi = \rho_e \mu_e u_e (r/r_o)^2 ds \tag{8}$$

Then, to be more general in our study of the transformation, consider the transformation of the term

$$s(r_o/r)^n \, d\bar{C}_p/ds \tag{9}$$

which is the same as the term under the square root in (2) except that r_o/r is assigned a general power.

At the start of the pressure rise, s has a value s_o. The quantity s will grow but only slowly with respect to its initial value s_o because of the considerable run of boundary layer flow ahead of the tail region. In any case, it only indirectly involves pressure gradients so it seems reasonable to assign it the constant value s_o. The main activity is in the gradient term $d\bar{C}_p/ds$. Now

$$d\bar{C}_p/ds = (d\bar{C}p/d\xi)(d\xi/ds) \tag{10}$$

Then, using (8) we have:

$$d\bar{C}_p/ds = \rho_e \mu_e u_e (r/r_o)^2 \, d\bar{C}_p/d\xi \tag{11}$$

When (11) is introduced into (9) we have approximately

$$s_o(r_o/r)^n \, \rho_e \mu_e u_e \, (r/r_o)^2 \, d\bar{C}_p/d\xi$$

From (8) we can see that, for the initial part of the flow, s_o can be written as $\xi_o/\rho_e \mu_e u_o$ because in the present incompressible problem ρ_e and μ_e are constants. Then we have, after cancelling ρ_e and μ_e, the expression

$$\xi_o \, (r_o/r)^n \, (r/r_o)^2 \, u_e/u_o \qquad\qquad \xi \geq \xi_o \tag{12}$$

For two-dimensional flow r/r_o is replaced by unity, so the r-term does not enter. For axisymmetric flow (12) should reduce to the same form. It will only do so if the power n is equal to 2. However, in the original derivation of the extended Stratford equation, the power n was found to be unity. The plots in Figures 1a, 1b, and 1c show that the test results indicate the originally derived n = 1 being a better approximation than n = 2, as given by

the Levy-Lees transformation. In (12), while there is approximation in the value of ξ by replacing it with ξ_o, the rest of the transformation is exact. In view of the conclusion that n = 1 is a better approximation and the fact that the original extended Stratford equation, (2), is simpler in implementation than the Levy-Lees transformation, the former is adopted in the present study rather than the latter, as originally proposed.

If (2) is squared for convenience and the substitution $s \equiv (s/s_o)s_o$ is made, the following formula is obtained

$$\bar{C}_p^2 \, (s/s_o)^{0.8} \, (r_o/r) \, d\bar{C}_p/[d(s/s_o)] = 0.25 \, (10^{-6} \, u_o s_o/\nu)^{1/5} \qquad (13)$$

which also can be written as

$$(s/s_o)^{0.8} \, (r_o/r) \, d\bar{C}_p^3/[d(s/s_o)] = 0.75 \, (10^{-6} \, u_o s_o/\nu)^{1/5} \qquad (14)$$

In these forms it is seen that a significant constant is the Reynolds number of the equivalent flow at the start of pressure rise, that is $u_o s_o/\nu$. At the start s/s_o and r_o/r are unity and so, from (14), it is clear that $\bar{C}_p$ can begin to rise faster when the Reynolds number is higher.

Also when solutions are plotted in s/s_o variables, for the two-dimensional case ($r_o/r = 1$) it is clear that the solutions are functions only of $u_o s_o/\nu$, and this quantity enters only weakly because of the 1/5th power exponent. If r_o/r were related uniquely to s/s_o, solutions would still be functions only of $u_o s_o/\nu$. In fact, r/r_o is indeed roughly a function of s/s_o. Equations (13) or (14) are useful because they show that if s_o is very small, a tail may be very short; if s_o is larger, the tail must be longer.

IMPLEMENTATION OF THE EXTENDED STRATFORD EQUATION

When first considering the problem of how to find a Stratford tail shape, our attention was given toward a direct approach of assuming a tail shape and then evaluating the resultant K, the L. H. S. of equation (2), as a function of s along the tail. Using the Douglas-Neumann potential flow program, numerous tail shapes of the following family were investigated

$$r(x)/r_o = \{[1-(x/L)^m]/[1+C(x/L)^n]\}^p \qquad (15)$$

This equation reflects a 5 parameter family of tails which intuitively has the necessary qualifications for at least approximating a Stratford type of flow. Although an invaluable degree of insight was obtained in examining this family, the large number of parameters proved to be overbearing in trying to develop a systematic approach for obtaining a reasonable approximation. In fact, any analytic expression for r(x) could, at best, lead only to an approximation of the desired flow. This fact is especially evident when it is realized that a few free parameters must exist to accommodate Reynolds number, transitional effects, forebody effects, and so on.

As is pointed out in the preceding section, the extended Stratford equation, (2), is a first order, non-linear differential equation if the relation $r(s)/r_o$ is known. However, finding the relation for $r(s)/r_o$ is precisely the end result sought. Hence, solving (2) by itself is somewhat enigmatic in that a functional coefficient in the differential equation is unknown.

In addition, the solution, if found, must also obey the laws of low speed fluid mechanics. Hence, it seemed that the appropriate course of action would be to couple the extended Stratford equation with a potential flow solution.

In light of this, an investigation was conducted into the application of Bristow's (Reference 10) inverse axisymmetric potential flow method which is an adaptation of the Douglas-Neumann potential flow program. Briefly stated, Bristow's method uses linear elements (actually cone frustums) with constant strength singularities to solve the potential flow problem directly. The resultant pressure (or velocity) distribution is then compared to some prescribed distribution and the body shape is systematically varied until the computed pressure matches the desired value. Bristow's method may be expressed functionally as

$$r = r\,[C_p(s)] \tag{16}$$

Realizing that equation (2) is equivalent to

$$C_p = C_p\,[r(s)] \tag{17}$$

then the iteration scheme reported earlier is immediately suggested. Of course in an iteration such as this, convergence is by no means guaranteed. Furthermore, it is not obvious from the above relations that all boundary conditions and other constraints (e.g., tail closure) can be simultaneously satisfied. Nevertheless, the first attempts at combining the equations (16) and (17) into one concurrent iteration procedure led to very encouraging results. Many solutions for various forebody and flow conditions were obtained, demonstrating that the overall concept is indeed a viable procedure.

In order to evaluate Stratford flows properly, it is necessary to incorporate some sort of boundary layer calculation on the forebody to extract θ_o and thence s_o, which appears explicitly in the extended Stratford equation. Since adapting or developing an advanced boundary layer computational procedure was inconsistent with the approximate nature of the extended Stratford equation, the simple but accurate momentum integral technique of E. Truckenbrodt was employed. His method can be found in several references (for instance, see Reference 11) and is repeated here for completeness. Given an axisymmetric body defined by r(s), the fluid velocities, freestream Reynolds number and transition station, s_t, the Truckenbrodt method yields

$$\theta(s)/\ell = [c_1^* + (c_{f_T}/2)^{7/6} \; I_T(s)^{6/7}/[(u/u_\infty)^3 \; (r/\ell)] \qquad (18)$$

where

$$c_1^* = (c_{f_L} \; I_L^{1/2}/2)^{7/6}$$

$$I_T(s) = \int_{s_T/\ell}^{s/\ell} (u/u_\infty)^{10/3} \; (r/\ell)^{7/6} \; d\,(s/\ell)$$

$$I_L = \int_0^{s_T/\ell} (u/u_\infty)^5 \; (r/\ell)^2 \; d\,(s/\ell)$$

$$c_{f_L} = 1.328/(u_\infty \ell/\nu)^{1/2}$$

$$c_{f_T} = 0.455/[\log_{10} (u_\infty \ell/\nu)^{2.58}]$$

Since s_o is an equivalent flat plate turbulent run in a freestream velocity u_o, a simple flat plate momentum integral may be employed, i.e.,

$$\theta_o = 0.036 \; s_o \; (u_o s_o/\nu)^{-1/5}$$

or, rearranging,

$$s_o = (\theta_o/0.036)^{5/4} \; (u_o/\nu)^{1/4} \qquad (19)$$

No serious attempt has been made to calculate the drag of the bodies. On the other hand, since $\theta(s)$ has been evaluated along the entire length from (18), the following Squire-Young formula (Reference 12)

$$C_D = (2\theta_A/A)\,(u/u_\infty)^{(H+5)/2},\quad \theta_A = 2\pi r\theta \tag{20}$$

is employed to estimate the growth of drag along the body.

In the present boundary layer integral approach, the form factor $H = \delta^*/\theta$ is not computed. However, incipient turbulent separation typically occurs at a value of $H = 2$. Since incipient separation is the prime characteristic of Stratford flows, $H = 2$ was assumed and applied over the entire body. A consequence of this assumption is that the forebody drag distribution is somewhat approximate because H is more like 1.3 for the forebody but the distribution along the tail should be quite good. Furthermore, drag distributions (i.e., cumulative drag as a function of length) are usually only of academic interest except near the tail. The "thin boundary layer" assumption breaks down near the tail end and sometimes an extrapolation of C_D versus s is required to estimate total vehicle drag. As will be demonstrated in the section discussing the results, the C_D versus s curves are surprisingly well behaved to the very tail extremity.

It should be noted that the s_o term as predicted by (19) is an explicit term in the extended Stratford equation, (2). Also, the quantities u_o and θ_o used to compute s_o are greatly affected by the potential flow distribution. Hence, the entire boundary layer computation scheme must be included within the iteration loop to allow for updating s_o with each pass.

NUMERICAL CONSIDERATIONS

Before embarking into the area of finding axially symmetric Stratford tails, it is necessary to establish certain procedures for presenting the initial geometry data to the computer. The Bristow/Douglas-Neumann approach is to approximate the body with a small but sufficient number of discrete frustum elements of sources and sinks. Although the zero-normal-velocity boundary condition determines the strengths of the sources (sinks), it is up to the user to decide upon both the required number and their position. Generally speaking, it is desirable to have a large number of elements in regions of large longitudinal gradients. Since machine speed and capacity are large factors in a computation of this type, a sparse distribution of points in regions of small gradients is desirable. However, the element size should not change abruptly. A good rule of thumb is that neighboring elements should not change in length by more than the ratio of the square-root of 2, i.e.,

$$\Delta s_{i+1} = \Delta s_i \times 2^{1/n}$$

where $n = \pm 2$.

While this relation is only a guideline, it does indicate that some means of clustering elements will usually be necessary, particularly for shapes of high fineness ratios. As an example, consider the hemisphere-cylinder-tail configuration. Since the hemisphere and tail will require a large number of elements, the above rule dictates that the elements at both ends of the cylinder be

fairly dense. In order to automate the clustering procedure, a "clustering function" for the cylinder was devised as follows:

$$H = C_1\, t + (1-C_1)\,[1-\cos(\pi t)]/2$$

$$x = x_{c_o} + H\,(x_{c_n} - x_{c_o})$$

$$y = r_o = \text{constant}$$

x_{c_o} = cylinder beginning

x_{c_n} = cylinder end

In this expression, t is uniformly spaced in the unit interval (Δt=constant) and the elements will be clustered near the cylinder endpoints. The degree of clustering is governed by the input parameter, C_1, where

$$0 < C_1 \leq 1$$

For the elliptic or Reichardt shapes, the situation is somewhat different. Defining these bodies parametrically will automatically cluster in regions of high curvature. For example, the Reichardt shapes reported herein were generated with the following equations:

$$x = b - b\cos t$$

$$y = a \sin^{2n} t$$

$$n = 0.42 \qquad \text{(for Reichardt bodies)}$$

The above equations will, in general, not place enough points at the aft end where high resolution is desired. Hence, a second parameter, ψ, is introduced as

$$t(\psi) = \pi\,[(2-C_1)\,\psi + (C_1-1)\,\psi^2]$$

where, as before, ψ is evenly spaced over the interval [0, 1] and C_1 is the

clustering parameter. For

$$1 < C_1 < \infty$$

the points will be clustered near the base.

The next immediate problem is to establish the tail portion of the geometry before any iteration begins. In our present study, there are two classes of solutions, the fixed forebody-geometry and fixed forebody-velocity types, and therefore, two classes of tail guesses are required. If the forebody is to remain essentially fixed, it is desirable to guess a tail shape as close to the final shape as possible. Subsequent iteration should then not appreciably alter the forebody. Our experience in using (15) has shown that a good initial guess for a tail on this class of bodies can be simplified to

$$r(x)/r_o = [1-(x/L)^{1.5}]/[1+(x/L)^{1.5}] \qquad (21)$$

As will be presently demonstrated, the tail length parameter, L, will always be a free parameter and finding the proper value becomes part of the solution process.

In the case of the fixed forebody-velocity shapes, a satisfactory initial tail guess cannot be effected as this will greatly disturb the upstream velocity. Instead, it is necessary to choose some point, s_r, on the unmodified shape and apply the extended Stratford recovery from that point aft. It is best to choose this point near the end but still in the constant velocity region of the flow. Other than this criterion, the choice of the point is completely arbitrary. However, that portion of the remaining arc length will generally not result in a converged tail solution. Furthermore, because of the clustering, the element spacing at the very trailing edge will

be very dense and may lead to numerical difficulties. As a result, it was found necessary to do two things to the tail portion of the constant velocity family:

1) equally space the elements aft of s_r, i.e.

$$\Delta s_i = \text{constant}$$

$$\text{for } i_o < i \leq N$$

2) introduce a multiplicative stretching factor, M, such that

$$\Delta s_{i_{new}} = M \cdot \Delta s_{i_{old}}, \quad i_o < i \leq N$$

The above modification must be done after the velocity distribution has been established. The stretching factor, M, is analogous to the tail length, L, in (21) and finding its proper value is likewise part of the solution.

The results presented herein were obtained using the above-mentioned procedures. They are indeed solutions to the combined potential flow problem and the extended Stratford equation. Unfortunately, obtaining such solutions is not exactly straightforward. There exists a very subtle problem in the nature of the solution, which thus far has not been satisfactorily resolved. Consider the extended Stratford equation, (7), and what is known prior to its integration. Since the geometry has been guessed (or inversely computed for each iteration), r(s) is known as well as the required initial conditions from the potential flow solution. Hence, (7) can be straightforwardly integrated. However, there exist certain additional requirements that cannot be directly imposed. If the tail extremity is denoted by t.e., then the requirement that $r_{t.e.} = 0$ must be met. From (7) it is also noted that $(d\bar{C}_p/ds)_{t.e.} = 0$. It is well known from potential flow theory that for this to happen at a non-zero velocity, $(dr/ds)_{t.e.} = 0$ (i.e., the tail must be a pure cusp). These requirements do not make the problem insoluble but do compli-

cate it tremendously. The difficulty arises from the fact that the location of the tail extremity, where these requirements are imposed, is not known a priori. Hence, the big remaining problem can be succinctly stated:

"Find the tail length that results in $r_{t.e.} = 0$"

Thus far in our investigation, no methodical way of doing this has been determined.

To put the problem in another way, the arc-length along the tail, $s_t = s_{t.e.} - s_o$, is established at the outset by the initial guess. The odds that a realistic solution will result are virtually nill. Particularly frustrating is the fact that the computed geometry will usually gyrate wildly during the iteration process. Assume for a moment that a bad guess has been made on s_t. After some 15 iterations or so, the geometry will be in total disorder and there is absolutely no indication on whether the guessed s_t resulted in a tail that is too long or too short. It has been our experience that there exists a narrow band on s_t such that whether s_t is too long or too short is clearly evident. If the value of s_t is in this band, then the following behavior is usually observed:

1) If s_t is too short, the tail will start toward the axis, but then flair out. It is smooth and resembles a rocket nozzle.
2) If s_t is too long, the tail arc will touch the axis and leave it for a short distance. It will be wrinkled near the end.

Our procedure has been to make a number of parallel computations in an effort to establish the band where appropriate corrective actions can be recognized. At this point it is a straightforward but possibly lengthy procedure to adjust the tail length until a meaningful solution results. For most of the cases presented herein, a solution was attained in six to eight tries.

On the other hand, there may be obstinate situations where an inordinate number of tries still result in failure. It is possible that solutions simply do not exist for some cases. This could be the result of choosing s_0 at a bad location on the body as in the fixed forebody-velocity situation.

The above-mentioned problems have been discussed primarily for two reasons. The first is to point out that the current solution procedure is not of a production nature. It takes a considerable expenditure in time and effort to obtain a single solution. The second reason is to indicate the difficulties associated with attempts to define an algorithm which will automatically converge on the tail length during the iteration procedure. The proper tail length indicator is completely absent (or very well disguised) in the mathematical problem. Also, the erratic behavior of the geometry and flowfield through the iterations defies any intuitive grasp of the situation which might otherwise suggest some automated procedure. Along these lines is the associated problem that a solution may not even exist and proof of existence is all but impossible. If a solution does exist, it may not be unique in the sense that slightly different tail lengths will still result in a solution such that the Stratford criterion is satisfied. In this context, the concepts of "precise" tail lengths and "optimizing procedures" become ambiguous.

In spite of the above complications, the "brute force" iteration technique which was employed led to many solutions that are presented in this report. The primary message is that the reported method usually will yield the desired end result of an axisymmetric Stratford tail, but with some difficulty.

DISCUSSION OF RESULTS

Having successfully developed a design procedure for finding Stratford tail shapes, some meaningful way of demonstrating the method was sought. Although the tail is generally envisioned as an appendage to some forebody, it will slightly alter forebody pressures through its upstream influence. In addition, because this particular problem is solved with an inverse Neumann procedure, the entire forebody shape is slightly altered by the addition of a tail. Also, because of the nature of the extended Stratford equation, the forebody shape and its boundary layer characteristics have a strong influence on the final tail shape. In conclusion, the tail design is not a problem separable from the forebody design. Thus, for purposes of demonstration, two distinct families of solutions are identified. The two families can be loosely categorized as follows:

1. A prescribed forebody shape with the tail geometry being wholly defined by the Stratford recovery region.
2. A prescribed velocity distribution up to the point of the Stratford recovery.

To be still more specific, these two families were further narrowed down to two types. For the first family, a hemisphere-cylinder was chosen as this is somewhat representative of "conventional" torpedo designs. Various cylinder lengths are presented including a zero-length cylinder (i.e., a hemisphere-tail). For the second family, a constant velocity solution from the Reichardt

class of bodies was prescribed. Again, results are presented for various slenderness ratios.

Table 1 presents a summary of all cases computed under the guidelines established above. There are a total of 9 cases which were completed after the calculational procedure had reached a fully operational status. By "fully operational," it is meant that all new and necessary computational procedures were checked out and verified (e.g., the boundary layer computation, iteration procedures, etc.) and that a Stratford tail was achieved and validated. Each particular case in Table 1 is identified by a configuration code of the form CDX or RX. The CDX code signifies a constant-diameter body (hemisphere-cylinder) with X representing the length to diameter ratio of the basic forebody. One exception to this convention is the CD1 body (no cylinder section) which is simply called HEMI for hemisphere only. The RX nomenclature is used for the constant velocity shape which is from the Reichardt class of bodies. Again, X represents the slenderness ratio of the basic Reichardt body. Also presented in Table 1 are the pertinent flow conditions, such as the freestream Reynolds number based on body length and the state of the boundary layer on the forebody (laminar or turbulent), and the pertinent results.

As is pointed out in the preceding section, the final tail length is not known a priori as it is a function of Reynolds number, boundary layer state, and forebody geometry. Hence, for purposes of being consistent, the length parameter is a length referenced to some non-varying geometrical dimension of the body. For the CD class of bodies, the reference length was chosen as the distance from the nose to the end of the cylinder. In the case of the HEMI body, this reduces to the hemisphere radius. For the R class of bodies, the

reference length is that of the unmodified Reichardt geometry (fore and aft symmetry). Alternately, for CDX and RX bodies, the reference length is simply X diameters.

Since the boundary layer momentum thickness plays such an important role in the determination of the final tail shape, a test case was prepared from case no. 1 and checked using the more exact Cebeci-Smith boundary layer method (Reference 4) as implemented in the TAPS computer code (Reference 13). The results of this test case are presented in Figure 3. As can be seen, the momentum thicknesses as computed by the two methods are in remarkably good agreement. The most crucial value for θ is θ_o which determines s_o by (19). The θ_o point in Figure 3 occurs exactly at the minimum just aft of s/r=16. Here, the two computer programs are in such good agreement that the result seems almost fortuitous. Judging from the overall trends in the two curves, the Bristow/Truckenbrodt method appears to be more than adequate for serious design applications.

For comparative purposes, a similar momentum thickness distribution for the R8 body is presented in Figure 4. The significant message to be gained from Figure 4 is the manner of boundary layer growth as compared to the constant diameter CD8 body. As a consequence of the conservation of mass in axi-symmetric flows [r(x) effect], the boundary layer growth on Reichardt shapes is inhibited everywhere forward of the maximum diameter point. Aft of this point, the thickness begins to increase more rapidly, such that by the time the Stratford recovery begins, the boundary layer is quite thick relative to a constant diameter body. In contrast, the boundary layer development on constant diameter bodies has a more or less flat plate behavior until the

flow begins to accelerate near the tail juncture. From (18) it can be seen that locally (for small variations in s), θ varies inversely as $(u_e/u_\infty)^3$. Since (u_e/u_∞) is not constrained in the constant diameter solutions, θ will minimize at the tail juncture where, by definition, θ_o and s_o are determined.

This localized thinning effect has a very interesting feedback influence on the tail length for the constant diameter bodies. The reduction in θ_o promotes smaller values of s_o as seen by (19). Due to the nature of the extended Stratford equation as discussed previously, smaller s_o values tend to drive the tail length still shorter. The shorter tail lengths in turn produce still higher corner velocities and smaller values of θ_o. Thus, we have the pleasantly surprising result that the combined effects of the extended Stratford equation, the potential flow relations and boundary layer equations have a built-in "forcing function" that results in extremely short tails. This forcing function is even more pronounced in the case where the forebody is laminar since the momentum thickness is much smaller.

Two converged solutions that graphically indicate these effects are depicted in Figure 5. The two solutions are from cases 1 and 2 which are for the CD8 body at a Reynolds number of 10^7. The only difference is that case 1 is for a fully turbulent forebody while case 2 is laminar up to the tail juncture. As can be seen, the boattails for both cases are quite short and the pressure recovery exhibits a typical Stratford behavior. In taking a cursory look at the laminar flow body, the tail is so short that it intuitively invites disbelief. Its shortness is directly attributable to the combined effects of small θ_o, the resultant small s_o, and the deep pressure spike leading into the pressure recovery. All of these parameters are presented in Table 1 for

a case to case comparison. In either case, it is doubtful that these shapes, which satisfy the extended Stratford criterion, would be conceived and arrived at through experimental or trial-and-error numerical procedures.

To further validate the reported procedure of finding Stratford tail shapes, two other cases of fixed forebody geometries are presented in Figures 6 and 7. Figure 6 is a constant diameter L/D = 4 body. In this example, the forebody is laminar and the Reynolds number is 10^6. For this case, the tail length came out somewhat longer (in terms of maximum body radius) than the CD8 body. This result is directly attributable to the reduced Reynolds number of the flow. Referring to Table 1, the computed value for s_o on the CD4 body at $R_{e_L} = 10^6$ is 0.906 R, whereas on the longer CD8 body at $R_{e_L} = 10^7$, s_o is 0.448 R. The larger value for s_o, when coupled with the extended Stratford equation, requires a longer tail.

Figure 7 is a hemisphere followed immediately by a Stratford recovery tail. This case was computed at a relatively low Reynolds number, 10^6, with a fully turbulent forebody. This results in probably the longest tail necessary. That is, higher Reynolds numbers and/or some forebody laminarization could operate with a still shorter tail using the extended Stratford guidelines. Even for this case, however, the true L/D of this body is only 1.1. Furthermore, the solution was obtained with relative ease which indicates that still blunter forebodies (e.g., oblate spheroids) could be closed using the Stratford recovery method.

Thus far, all the cases discussed are of the "prescribed forebody" type. As was evident in the figures, this approach will almost invariably lead to deep, negative, pressure spikes at the tail juncture. In high speed underwater regimes, such low pressure areas may be intolerable from a cavitation standpoint. To alleviate this problem, the present method allows for constraining the forebody velocity up to the beginning of the pressure rise. One of the classical high speed underwater shapes is the Reichardt body. This geometry has a surface velocity that is nearly constant and nowhere exceeds the freestream velocity by 5 to 10 percent or so. Thus, it was felt that the Reichardt shapes would be good candidate bodies for applying the Stratford recovery method for tail design.

Figure 8 presents the results of applying the present method to Reichardt bodies of an initial L/D of 8. Two cases (3 and 4 in Table 1) are included in the figure. The only initial conditions that are different is that case 3 has a fully turbulent forebody while case 4 is laminar up to the start of the pressure rise. As is evident in the figure, the present method of coupling the extended Stratford equation with an inverse Neumann solution allows for maintaining the constant velocity up to the point of the Stratford recovery. When applied in this mode, however, the geometry of the forebody will be noticeably modified for several diameters forward of the point where the pressure rise begins. This is because of the elliptic nature of the potential-flow equation and will always occur when a velocity change over a limited region is required.

Also evident in Figure 8 is that the start of the pressure rise does not occur at exactly the same station for the two cases. The reason is twofold. First, where the pressure recovery starts in a constant velocity region is an arbitrary choice. Second, the length of the tail may influence the required density of source/sink elements on the tail such that sufficient definition of the flow is attained. This latter effect has to do with the numerics of the problem as discussed in the preceding section.

Some of the important output parameters from the two cases are summarized in Table 1. For example, the computed values of s_o for the R8 configurations (cases 3 and 4) are considerably larger than their counterparts on the CD8 bodies (cases 1 and 2). As discussed earlier, this is due to the extensive thickening of the boundary layer on the aft end of Reichardt shapes. In addition, the lack of high velocities that are permitted in cases of fixed forebody geometries is a contributor. These effects are reflected in the tabulated values of θ_o, C_{pmin} and $u_o s_o/\nu$.

In order to assess the impact of Reynolds number on tail design, the Reynolds number of 10^7 in case 3 is complemented by cases 5 and 6 which are at Reynolds numbers of 10^6 and 10^8 respectively. The afterbody shapes and pressure distributions from these cases are presented in Figure 9. The significant conclusion to be made from this example is that tail shapes in fully turbulent flows are not appreciably affected over a wide range of Reynolds numbers. Thus, a tail that is optimally designed for the lower end of the anticipated Reynolds number spectrum should not degrade in performance with increasing Reynolds number. Alternately, if the design process has some

built-in conservatism, e.g., a reduced value of K in equation (2), then Reynolds number should not play an important role in tail design. Of course, all of these statements are predicated on the assumption that the forebody will remain turbulent. If the forebody should become laminar, the tail will simply be off-design, but conservative and will not have separated flow.

Figure 10 is a plot of the computed values of θ_o, s_o, and C_D versus Reynolds number for the three cases just discussed. One interesting result in this figure is that s_o comes out nearly double the total body length. This is a characteristic of Reichardt shapes as discussed several times previously. The drag coefficient for these and all other cases is given in the form $C_D A/R^2$ for ease in extracting C_D for various reference areas. For example, to obtain C_D referenced to frontal area, divide $C_D A/R^2$ by π. To obtain C_D referenced to the two-thirds power of the volume, divide $C_D A/R^2$ by $V^{2/3}/R^2$ which is tabulated for all cases in Table I.

In a report by Hess and James (Reference 14) entitled "On the Problem of Shaping an Axisymmetric Body to Obtain Low Drag at Large Reynolds Numbers", there are several conclusions which we would like to quote verbatim.

a. A shape having the lowest drag at one Reynolds number has the lowest drag at all Reynolds numbers.
b. *Shapes with fineness ratios in the range of* 3 to 4 have the lowest drag coefficients based on the two-thirds power of the volume.
c. Drag coefficient is insensitive to shape and no shape has been found with significantly lower drag than a boattailed prolate spheroid. A more accurate drag calculation might modify these conclusions slightly, but would probably not drastically revise them.

In all, some 50 bodies were investigated by Hess and James and some of these bodies were of the constant velocity type described herein. Moreover, the boattails were merely streamlined to prevent separation and no optimization procedures were employed. Figure 11, which is taken directly from their report, is one example from which their conclusions were based. This figure is chosen for inclusion in our report since it portrays the drag behavior of modified Reichardt shapes (constant velocity shapes with a streamlined tail). One data point from our results is suitable for inclusion on this figure and has been added. It is for the R8 body of case 3 and indicates that a drag reduction is obtainable through proper tail optimizing procedures. The reduction is substantial and needs to be verified. However, tails on all the other bodies in the figure were conventional. This one, being mostly concave, may indeed demonstrate the drag reduction that has been calculated.

The last geometry to be reported is from case no. 8. This is the R4 configuration at a Reynolds number of 10^6 with a laminar forebody. Although this particular case was primarily included as a further substantiation of the reported method, it does have some interesting attributes. For example, C_D based on the two-thirds power of the volume is only 0.0098. Although some of the longer shapes have smaller C_D values, it is because laminar flow was assumed to exist at a Reynolds number of 10^7. A long laminar run at this Reynolds number would be very difficult to maintain. Hence, for practical application, the R4 laminar flow body is a good candidate configuration where drag is of primary concern. In fact, the tail optimization procedure could be exercised for a variety of forebody shapes in an attempt to minimize overall drag. Furthermore, the method is not restricted to an underwater regime and the concept is equally applicable to two-dimensional flows as well.

Thus far, we have presented what we consider to be the most fruitful results of our study. From what we can perceive, the extended Stratford equation and associated numerical procedures do indeed lead to a very short tail with incipient separation being sustained from the start of the pressure rise to the trailing edge. Verification of all these results by using more exact methods of computation is desirable, but is not within the level of the present effort. Perhaps even more importantly, the only real proof of the existence of these types of flows lies in experimental validation. In the hope that we have stirred some interest in this area, computer generated tables of geometries for the 9 cases are included in Tables 2 through 10. Perhaps some interested readers will consider using these results in their own fields of endeavor.

REFERENCES

1. Stratford, B. S., "The Prediction of Separation of the Turbulent Boundary Layer." J. Fluid Mech., Vol. 5, No. 1, 1959.

2. Liebeck, R. H., "A Class of Airfoils Designed for High Lift in Incompressible Flow." Journal of Aircraft, Vol. 10, No. 10, 1973.

3. Liebeck, R. H., "Wind Tunnel Tests of Two Airfoils Designed for High Lift without Separation in Incompressible Flow." McDonnell Douglas Report MDC J5667-01, 1972.

4. Cebeci, T., and Smith, A.M.O., "Analysis of Turbulent Boundary Layers." Academic Press, New York, 1974, See Section 7.3.

5. Smith, A.M.O., "Stratford's Turbulent Separation Criterion for Axially-Symmetric Flows." Jour. of App. Math and Physics (ZAMP), Vol. 28, 1977.

6. Huang, T. T., Wang, H. T., Santelli, N., and Groves, N. C., "Propeller/Stern/Boundary-Layer Interaction on Axisymmetric Bodies. Theory and Experiment." NSRDC Report 76-0113, 1976.

7. Patel, V. C., "A Simple Integral Method for the Calculation of Thick Axisymmetric-Turbulent Boundary Layers." Aero. Quarterly, Vol. 25, Pt. I, 1974.

8. Nakayama, A., and Patel, V. C., "Calculation of the Viscous Resistance of Bodies of Revolution." Jour. Of Hydronautics, Vol. 8, No. 4, 1974.

9. Nelson, D. M., "Development of a Blunt Afterbody Configuration for the RETORC Torpedo." Naval Undersea Warfare Center Report NUWC TP-15, 1968.

10. Bristow, D. R., "A Solution to the Inverse Problem for Incompressible Axisymmetric Potential Flow." AIAA Paper 74-520, 1974.

11. Schlichting, H., "Boundary Layer Theory." McGraw-Hill, New York, 1968.

12. Young, A. D., "The Calculation of Total and Skin Friction Drags of Bodies of Revolution at Zero Incidence." ARC R&M No. 1874, 1939.

13. Gentry, A. E., "The Transition Analysis Program System." McDonnell Douglas Report MDC J7255, 1976.

14. Hess, J. L., and James, R. M., "On the Problem of Shaping An Axisymmetric Body to Obtain Low Drag at Large Reynolds Number." McDonnell Douglas Report MDC J6791, 1975.

15. Murphy, J. S., "The Separation of Axially Symmetric Turbulent Boundary Layers, Part I," Douglas Aircraft Report ES 17513, 1954.

16. Presz, W. M., Jr. and Pitkin, E. T., "Flow Separation over Axisymmetric Afterbody Models," Journal of Aircraft, Vol. 11, No. 11, 1974.

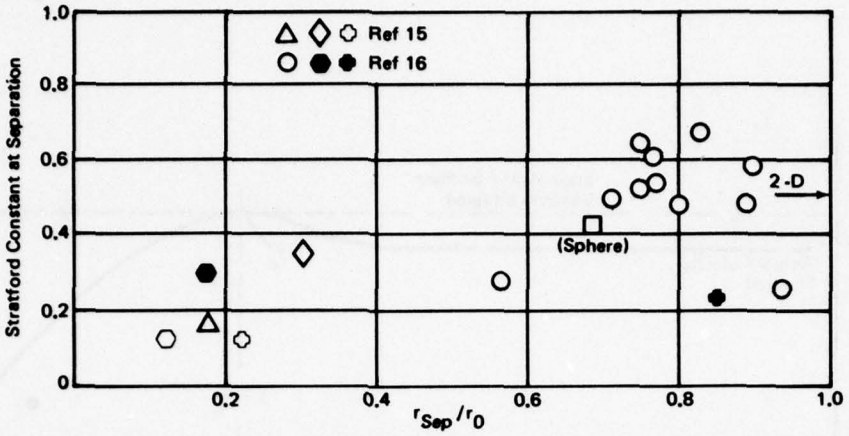

Figure 1a. Experimental Values of The Stratford Constant at Separation According to Equation (2) Without the r_0/r Term

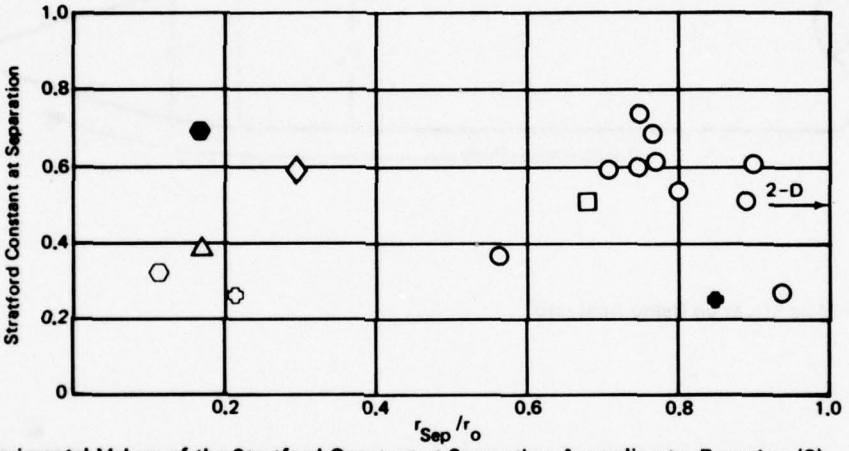

Figure 1b. Experimental Values of the Stratford Constant at Separation According to Equation (2)

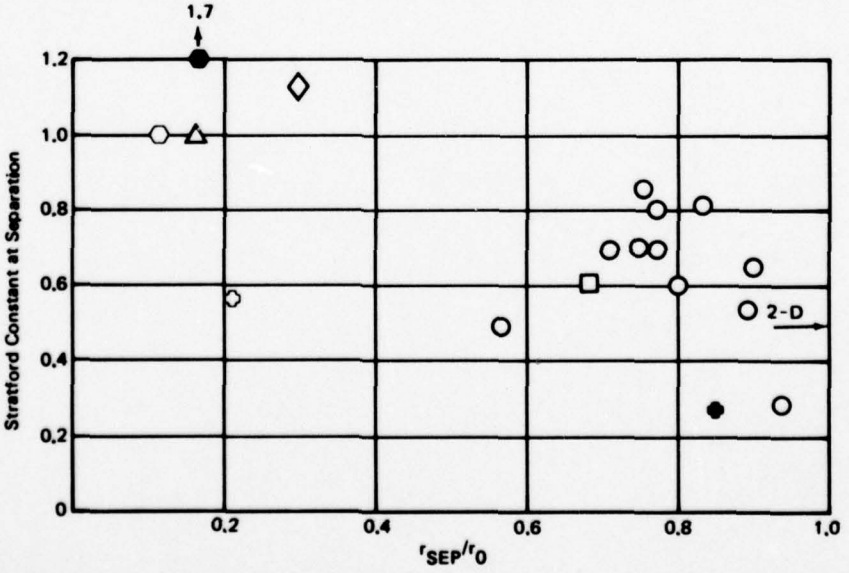

Figure 1c. Experimental Values of the Stratford Constant at Separation Calculated According to the Levy-Lees Transformation

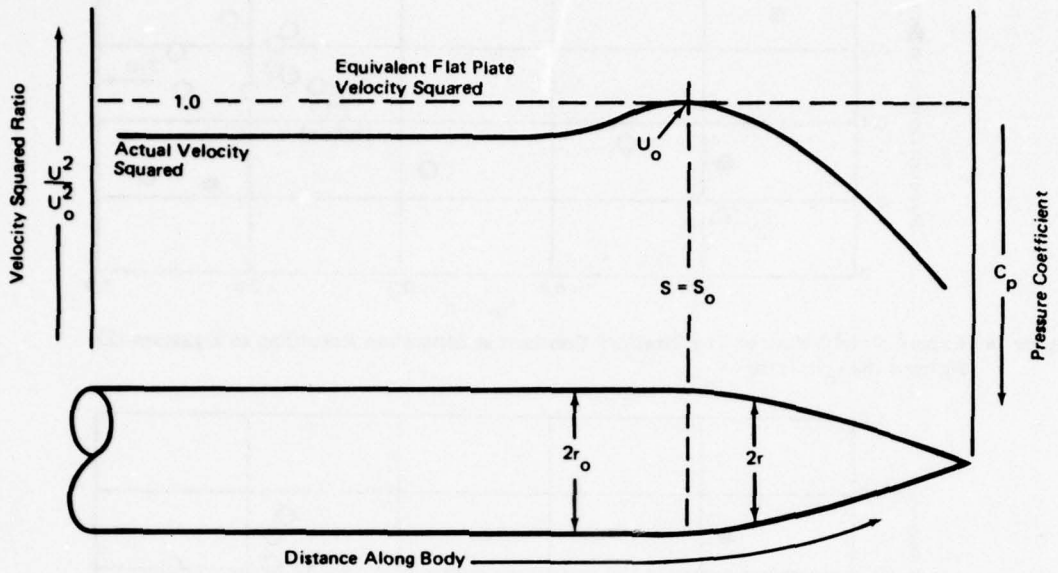

Figure 2. The Flow Situation Being Analyzed

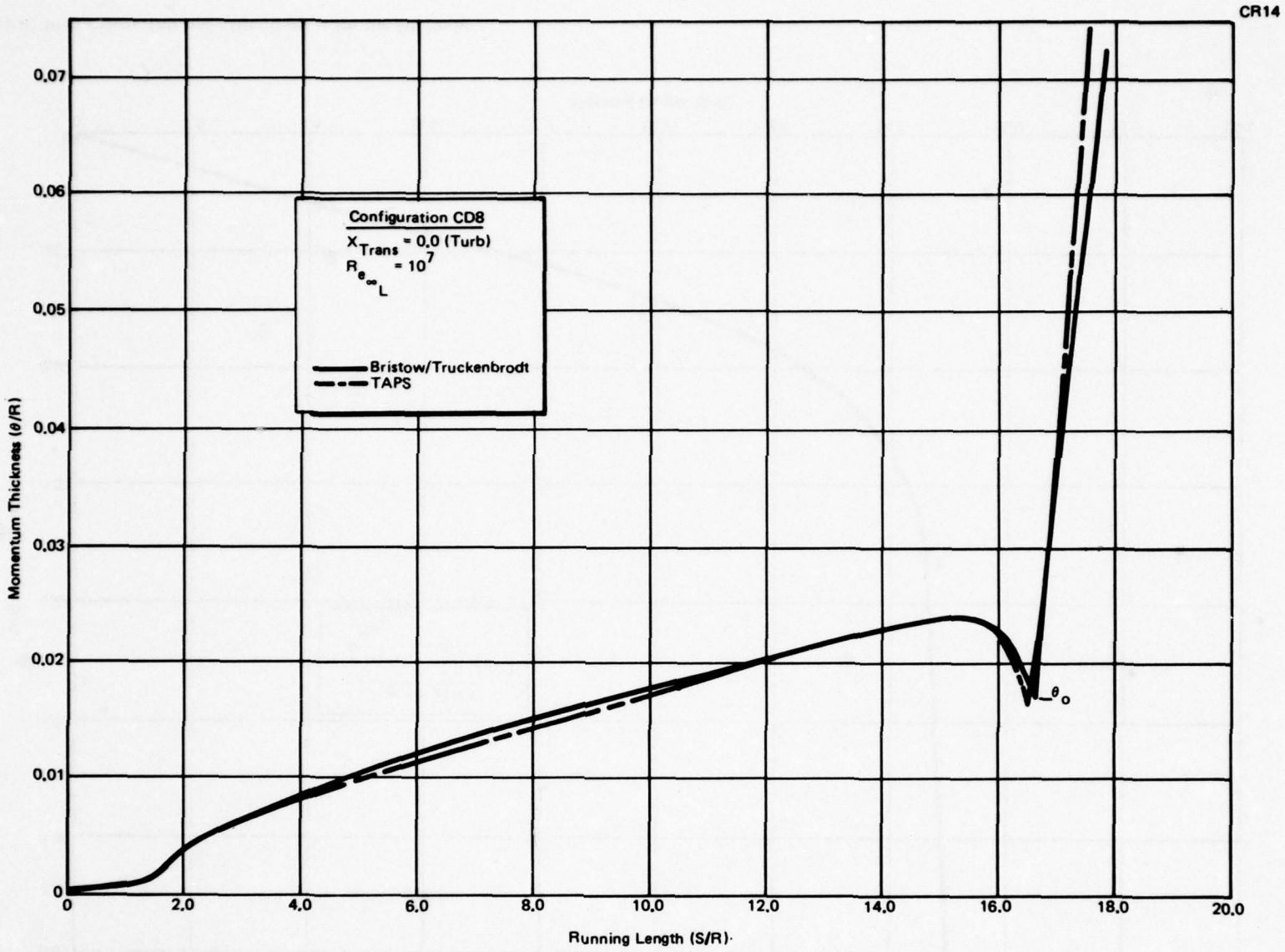

Figure 3. Comparison of Momentum Thickness Distribution Predictions for the CD8 Body

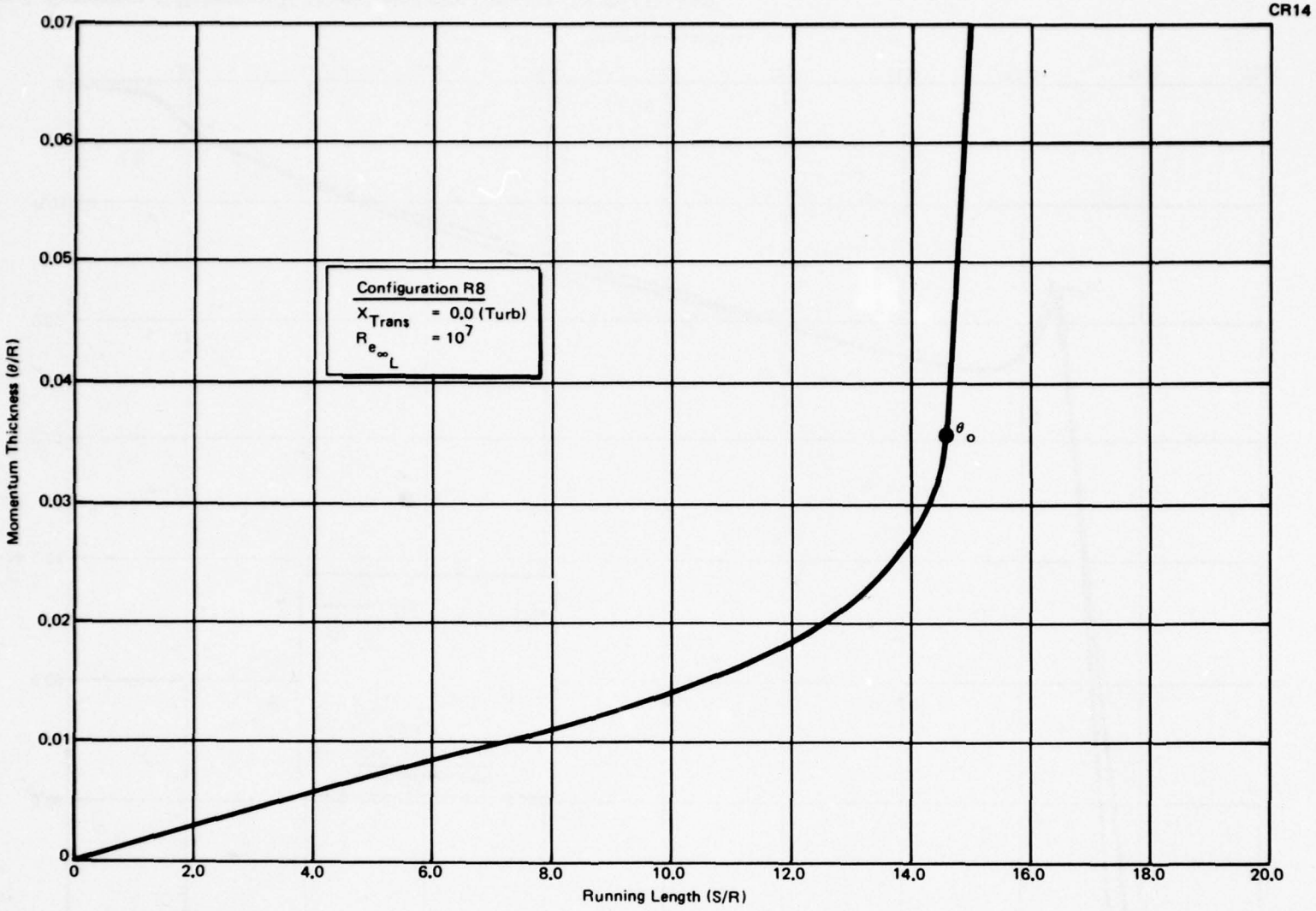

Figure 4. Momentum Thickness Distribution for the R8 Body

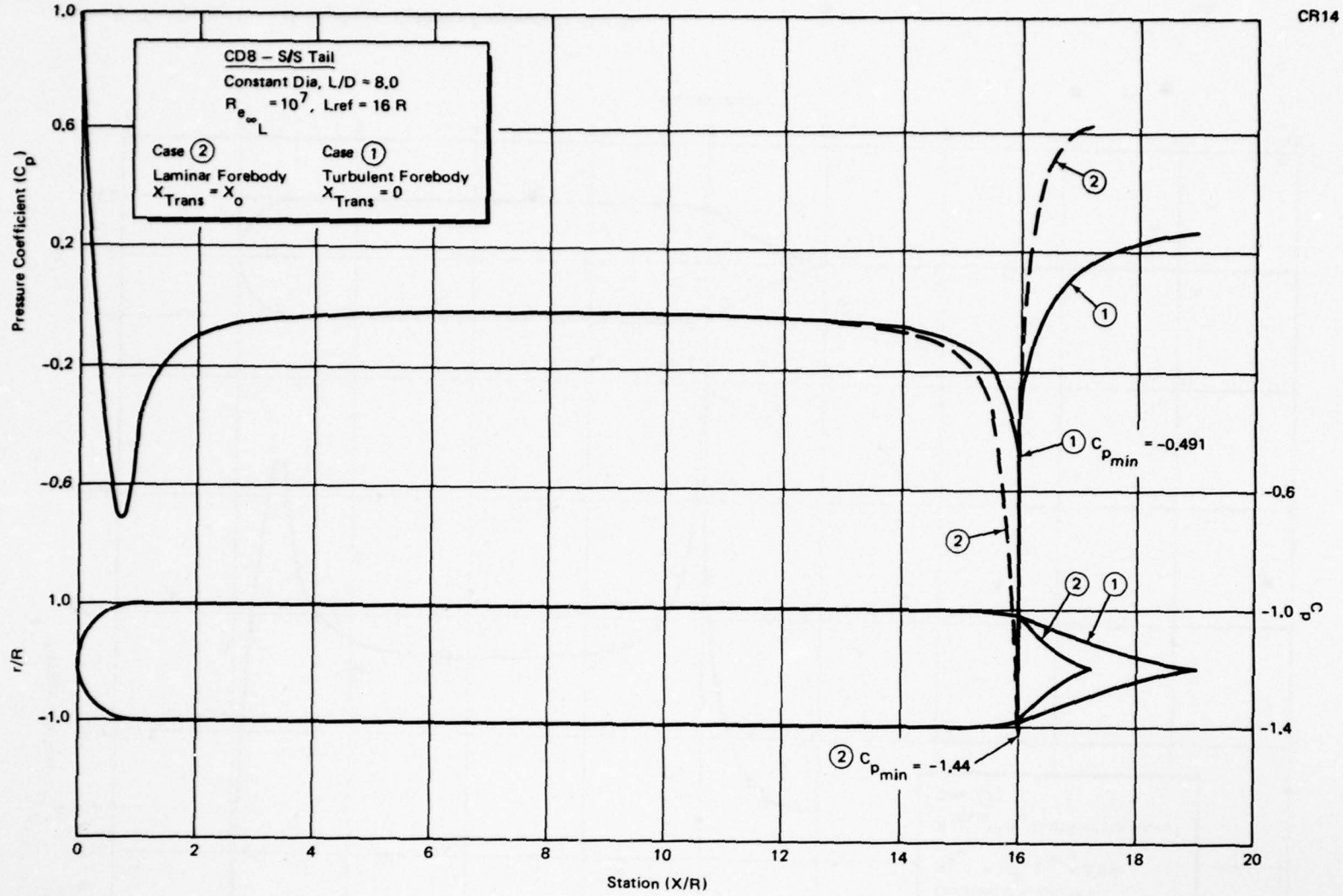

Figure 5. Tail Designs for Laminar and Turbulent Flows Over a Hemisphere - Cylinder Forebody (L/D = 8)

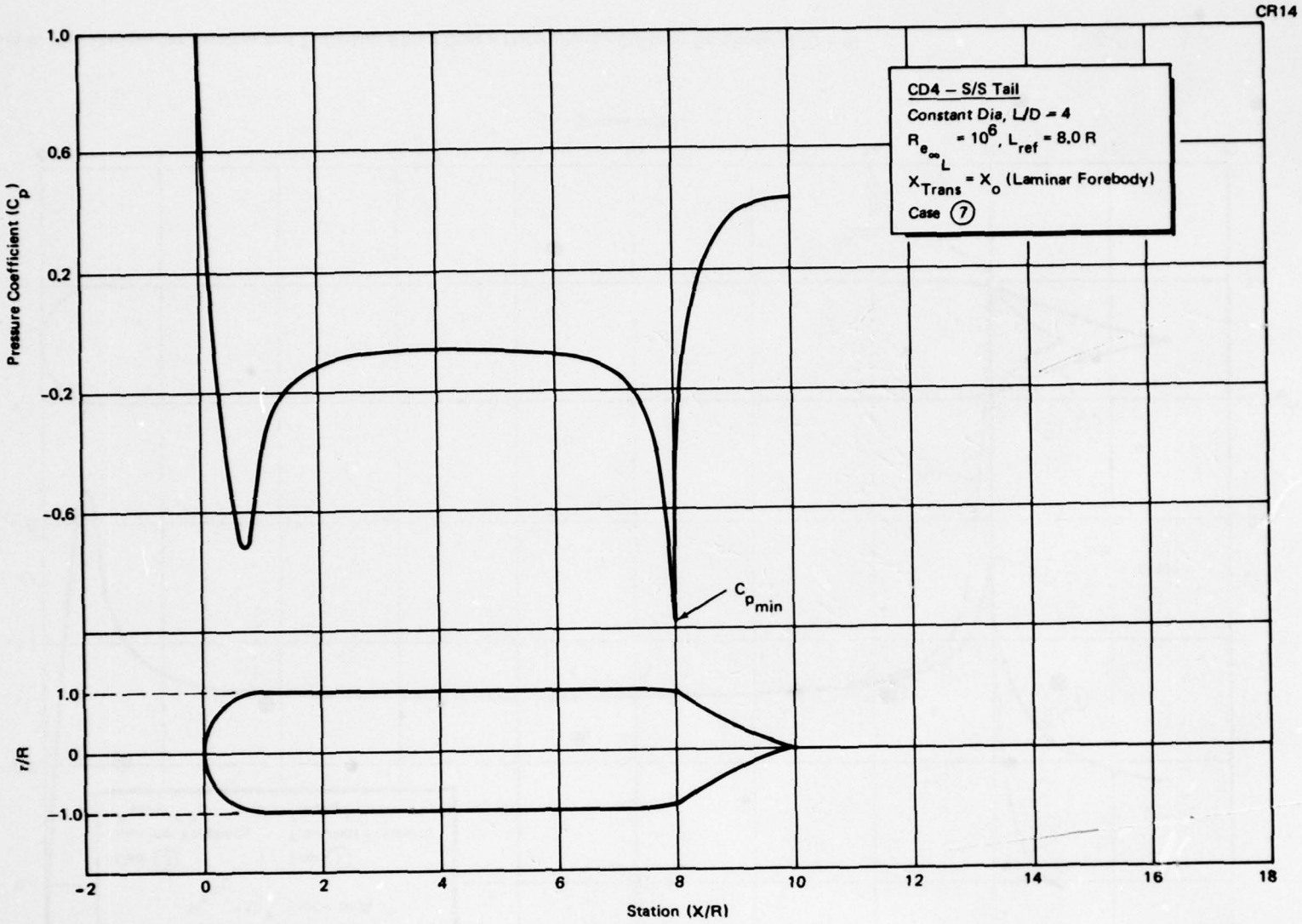

Figure 6. Tail Design for a Hemisphere - Cylinder Forebody (L/D = 4)

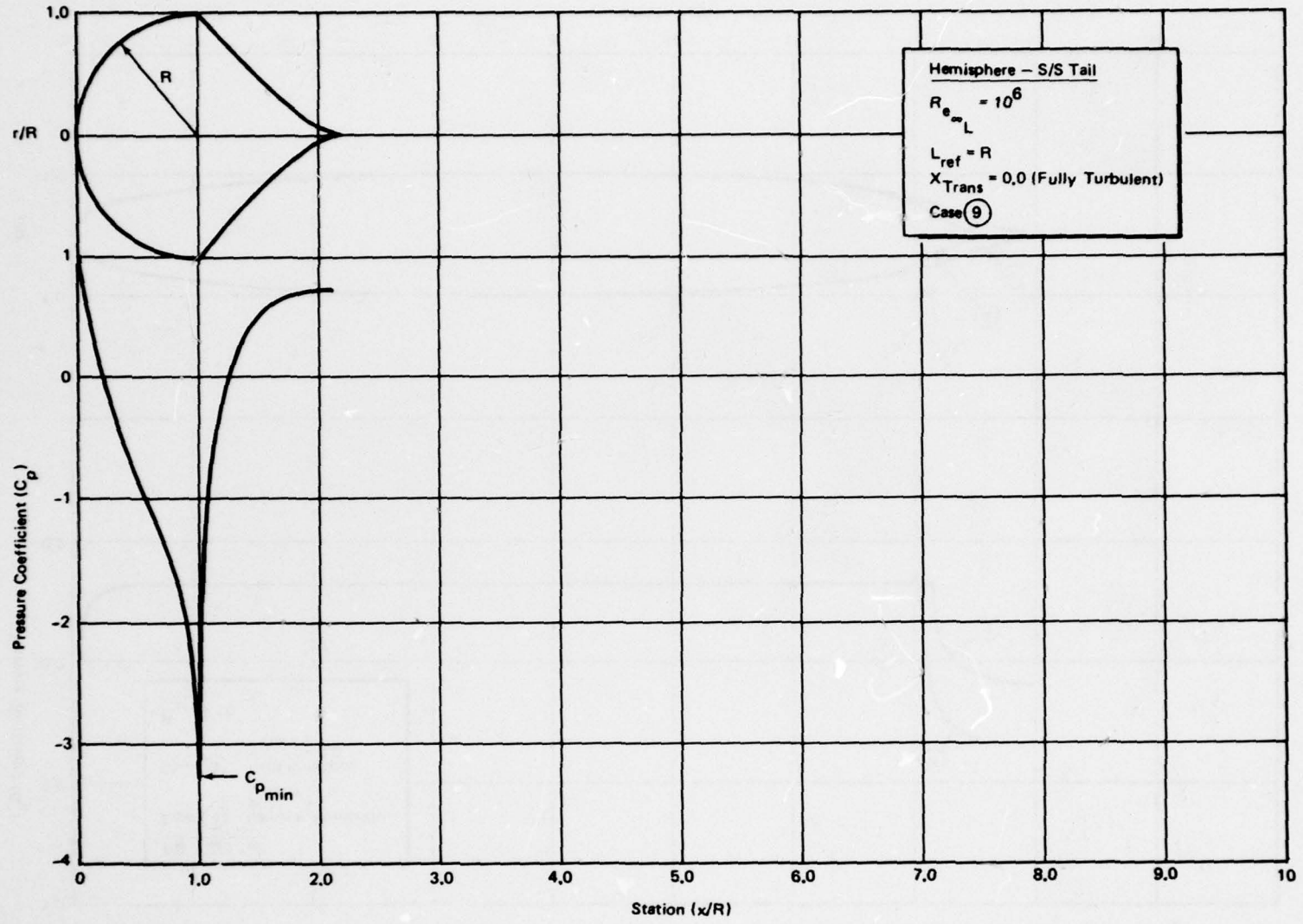

Figure 7. Tail Design for a Hemisphere Forebody

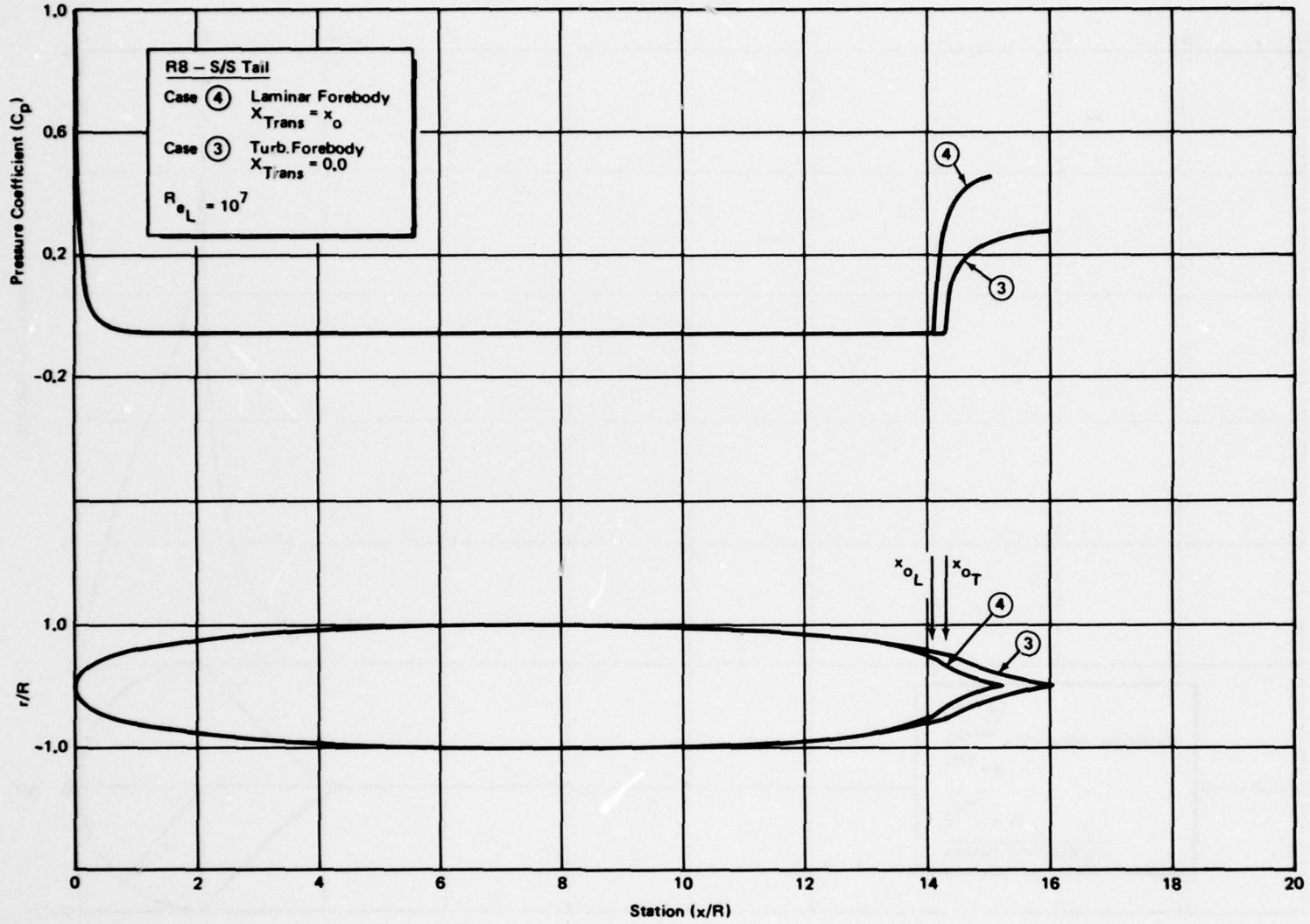

Figure 8. Tail Designs for a Reichardt Body

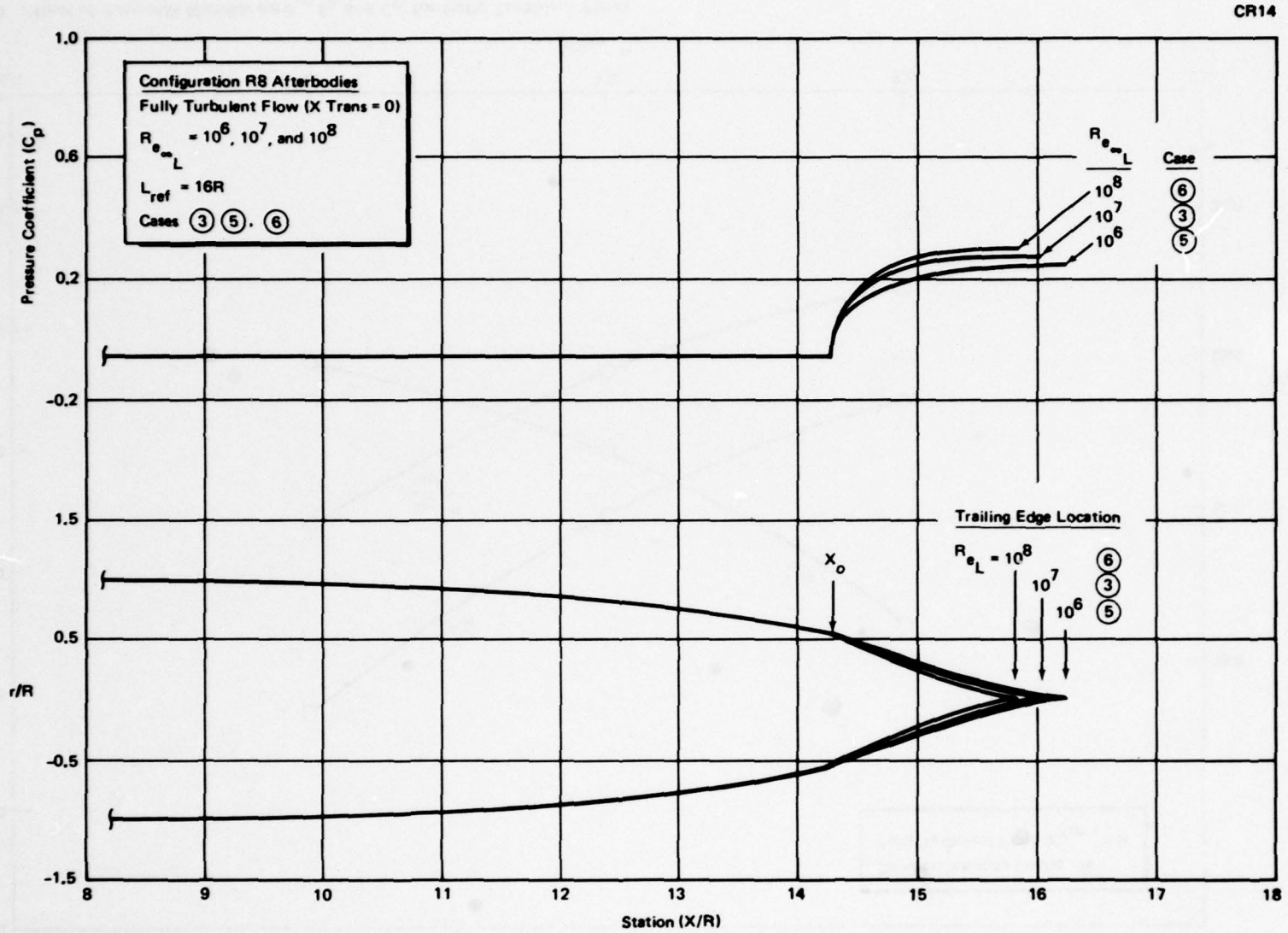

Figure 9. Effect of Reynolds Number on Tail Design for Fully Turbulent Flows

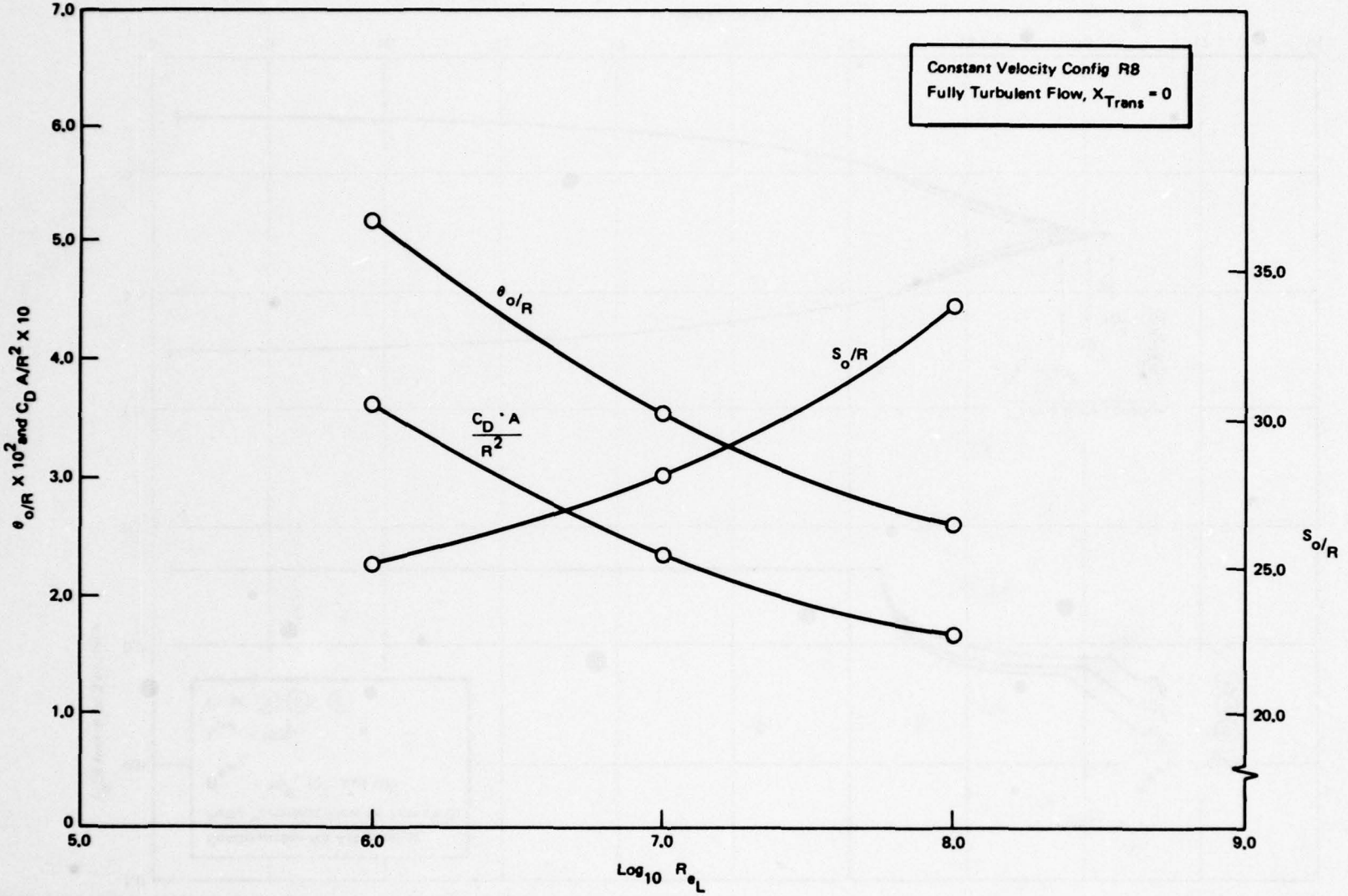

Figure 10. Effect of Reynolds Number on θ_o, S_o and C_D for Fully Turbulent Flows

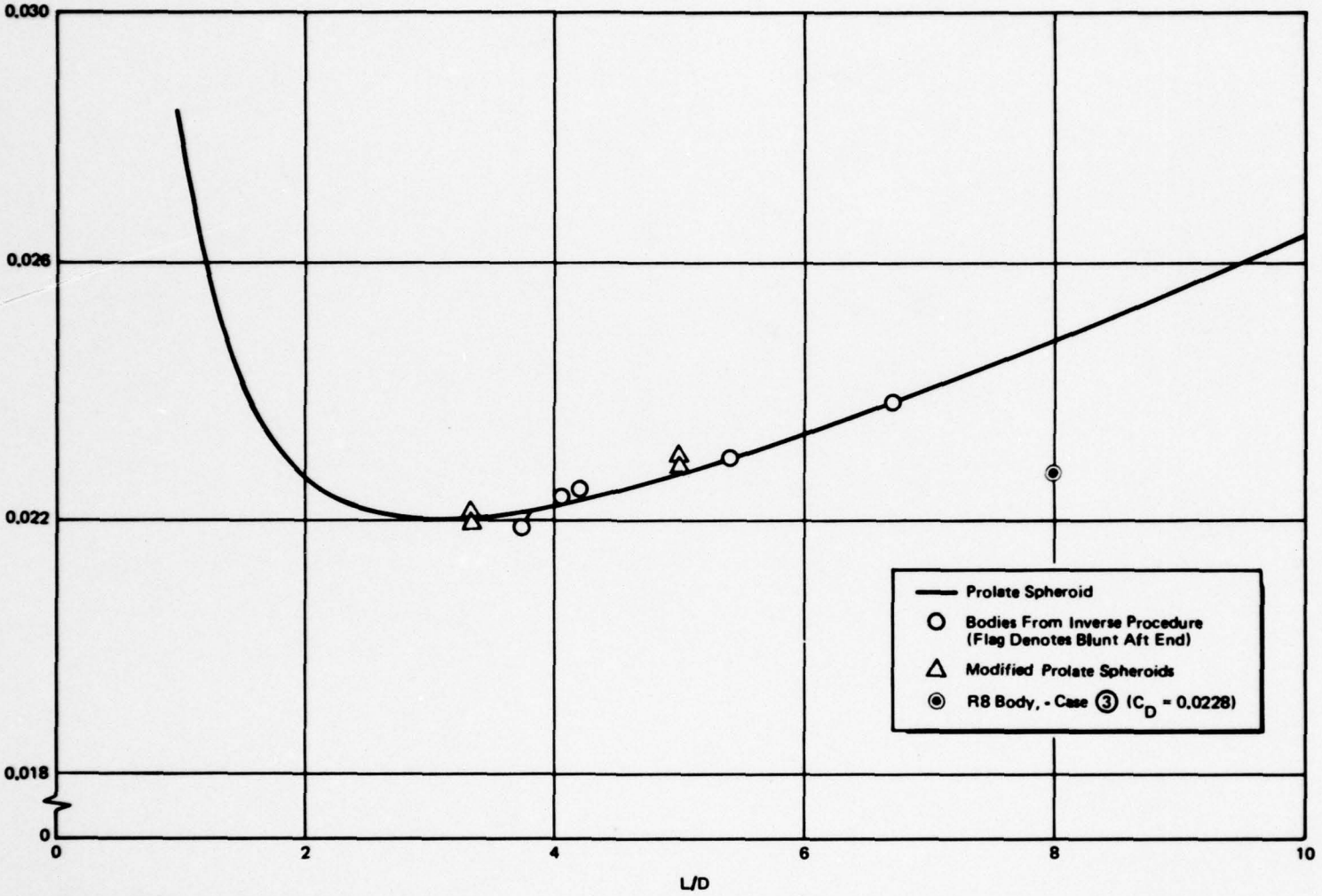

Figure 11. Calculated Drag Coefficients Versus Fineness Ratio for Constant-Pressure Bodies at a Reynolds Number of 10 Million

Table 1

Computation Schedule and Pertinent Output Parameters

No.	Configuration	Re_L	Forebody State		θ_o/R	s_o/R	s_o/L	$\frac{C_D \cdot A}{R^2}$	$\frac{V^{2/3}}{R^2}$	Tail Length TL/R	$\frac{u_o/s_o}{\nu} \times 10^{-6}$	$C_{P_{min}}$
1	CD8	10^7	Turb.		0.0170	11.59	0.726	0.344	14.30	3.10	8.847	-0.492
2	CD8	10^7	Lam.		0.00120	0.4485	0.28	0.0470	14.17	1.25	0.438	-1.437
3	R8	10^7	Turb.		0.358	28.11	1.75	0.239	10.51	1.77	18.10	-0.06
4	R8	10^7	Lam.		0.00583	2.91	0.182	0.0326	10.35	1 .015	1.88	-0.07
5	R8	10^6	Turb.		0.0518	25.13	1.57	0.362	10.61	2.02	1.62	-0.06
6	R8	10^8	Turb.		0.0262	33.89	2.12	0.167	10.51	1.58	218.2	-0.06
7	CD4	10^6	Lam.		0.00297	0.9062	0.113	0.0996	8.92	2.0	0.159	-0.98
8	R4	10^6	Lam.		0.00643	2.24	0.281	0.0657	6.74	1.50	0.309	-0.17
9	HEMI	10^6	Turb.		0.00087	0.361	0.361	0.0862	2.21	1.2	0.744	-3.26

Table 2

Case 1

CD8, TURB., $Re_L = 10^7$

I	X/R	r/R
1	0.0000	0.0000
2	.0093	.1566
3	.0426	.3100
4	.0999	.4561
5	.1797	.5912
6	.2798	.7120
7	.3977	.8156
8	.5303	.8994
9	.6746	.9613
10	.8266	.9999
11	.9829	1.0138
12	1.2397	1.0167
13	1.6332	1.0202
14	2.1585	1.0244
15	2.8072	1.0289
16	3.5679	1.0335
17	4.4266	1.0376
18	5.3667	1.0410
19	6.3696	1.0433
20	7.4154	1.0440
21	8.4828	1.0433
22	9.5503	1.0401
23	10.5961	1.0355
24	11.5990	1.0280
25	12.5391	1.0194
26	13.3977	1.0074
27	14.1583	.9955
28	14.8068	.9795
29	15.3319	.9656
30	15.7250	.9462
31	15.9814	.9336
32	16.1325	.8925
33	16.2782	.8266
34	16.4333	.7784
35	16.5871	.7207
36	16.7439	.6679
37	16.9007	.6127
38	17.0585	.5596
39	17.2163	.5066
40	17.3743	.4550
41	17.5322	.4045
42	17.6899	.3556
43	17.8474	.3081
44	18.0047	.2623
45	18.1618	.2182
46	18.3188	.1760
47	18.4756	.1358
48	18.6323	.0978
49	18.7890	.0624
50	18.9459	.0298
51	19.1032	.0022

Table 3

Case 2

CD8, LAM., $Re_L = 10^7$

I	X/R	r/R
1	0.0000	0.0000
2	.0089	.1567
3	.0419	.3101
4	.0939	.4563
5	.1784	.5916
6	.2783	.7126
7	.3960	.8164
8	.5285	.9004
9	.6726	.9625
10	.8247	1.0014
11	.9809	1.0155
12	1.2377	1.0189
13	1.6312	1.0228
14	2.1565	1.0277
15	2.8051	1.0330
16	3.5658	1.0385
17	4.4245	1.0436
18	5.3646	1.0480
19	6.3676	1.0514
20	7.4133	1.0531
21	8.4808	1.0534
22	9.5482	1.0512
23	10.5940	1.0472
24	11.5970	1.0404
25	12.5370	1.0320
26	13.3956	1.0204
27	14.1563	1.0077
28	14.8047	.9912
29	15.3298	.9745
30	15.7227	.9519
31	15.9784	.9294
32	16.0343	.8938
33	16.0821	.8376
34	16.1409	.7847
35	16.2009	.7275
36	16.2631	.6692
37	16.3266	.6102
38	16.3912	.5515
39	16.4566	.4940
40	16.5227	.4389
41	16.5893	.3841
42	16.6564	.3326
43	16.7240	.2838
44	16.7918	.2377
45	16.8599	.1945
46	16.9283	.1542
47	16.9969	.1169
48	17.0654	.0827
49	17.1344	.0518
50	17.2035	.0242
51	17.2736	.0024

Table 4

Case 3

R8, TURB., $Re_L = 10^7$

I	X/R	r/R
1	0.0000	0.0000
2	.0229	.1443
3	.0947	.2435
4	.2131	.3294
5	.3761	.4070
6	.5818	.4780
7	.8277	.5434
8	1.1115	.6037
9	1.4307	.6593
10	1.7824	.7104
11	2.1640	.7572
12	2.5727	.7997
13	3.0055	.8380
14	3.4596	.8722
15	3.9319	.9023
16	4.4198	.9283
17	4.9202	.9504
18	5.4305	.9685
19	5.9478	.9828
20	6.4695	.9932
21	6.9930	.9998
22	7.5160	1.0027
23	8.0359	1.0019
24	8.5507	.9975
25	9.0581	.9895
26	9.5563	.9780
27	10.0434	.9630
28	10.5176	.9445
29	10.9774	.9226
30	11.4214	.8972
31	11.8483	.8684
32	12.2570	.8359
33	12.6463	.7999
34	13.0153	.7596
35	13.3632	.7152
36	13.6892	.6652
37	13.9924	.6093
38	14.2712	.5426
39	14.4968	.4966
40	14.5365	.4360
41	14.6725	.3913
42	14.8069	.3417
43	14.9432	.2978
44	15.0793	.2534
45	15.2164	.2119
46	15.3537	.1714
47	15.4918	.1332
48	15.6302	.0966
49	15.7692	.0623
50	15.9088	.0303
51	16.0492	.0023

Table 5

Case 4

R8, LAM., $Re_L = 10^7$

I	X/R	r/R
1	0.0000	0.0000
2	.0139	.1222
3	.0601	.2071
4	.1381	.2815
5	.2472	.3496
6	.3870	.4129
7	.5569	.4723
8	.7561	.5281
9	.9840	.5808
10	1.2396	.6303
11	1.5219	.6769
12	1.8298	.7205
13	2.1620	.7612
14	2.5173	.7990
15	2.8942	.8337
16	3.2912	.8655
17	3.7068	.8942
18	4.1394	.9197
19	4.5872	.9421
20	5.0484	.9613
21	5.5213	.9771
22	6.0039	.9896
23	6.4944	.9988
24	6.9909	1.0043
25	7.4912	1.0065
26	7.9935	1.0049
27	8.4958	.9998
28	8.9961	.9906
29	9.4924	.9780
30	9.9827	.9608
31	10.4650	.9403
32	10.9375	.9144
33	11.3932	.8854
34	11.8451	.8496
35	12.2767	.8111
36	12.6906	.7631
37	13.0857	.7127
38	13.4584	.6470
39	13.8089	.5774
40	14.1273	.4744
41	14.2185	.4277
42	14.2994	.3647
43	14.3895	.3159
44	14.4789	.2658
45	14.5706	.2200
46	14.6632	.1760
47	14.7571	.1350
48	14.8521	.0966
49	14.9484	.0614
50	15.0457	.0292
51	15.1447	.0026

Table 6

Case 5

R8, TURB., $Re_L = 10^6$

I	X/R	r/R
1	0.0000	0.0000
2	.0229	.1443
3	.0947	.2435
4	.2130	.3295
5	.3761	.4071
6	.5817	.4782
7	.8276	.5437
8	1.1114	.6042
9	1.4305	.6601
10	1.7822	.7114
11	2.1638	.7584
12	2.5724	.8012
13	3.0052	.8398
14	3.4592	.8743
15	3.9316	.9048
16	4.4194	.9312
17	4.9198	.9536
18	5.4301	.9722
19	5.9473	.9868
20	6.4690	.9976
21	6.9926	1.0046
22	7.5155	1.0078
23	8.0355	1.0074
24	8.5502	1.0034
25	9.0577	.9958
26	9.5559	.9847
27	10.0430	.9700
28	10.5172	.9520
29	10.9771	.9305
30	11.4211	.9057
31	11.8480	.8773
32	12.2567	.8455
33	12.6461	.8100
34	13.0152	.7708
35	13.3632	.7272
36	13.6895	.6790
37	13.9929	.6244
38	14.2726	.5617
39	14.4233	.5133
40	14.5688	.4511
41	14.7202	.4049
42	14.8700	.3537
43	15.0216	.3083
44	15.1730	.2621
45	15.3253	.2192
46	15.4779	.1771
47	15.6311	.1374
48	15.7847	.0994
49	15.9390	.0638
50	16.0938	.0309
51	16.2494	.0022

Table 7

Case 6

R8, TURB., $Re_L = 10^8$

I	X/R	r/R
1	0.0000	0.0000
2	.0228	.1444
3	.0945	.2435
4	.2128	.3296
5	.3758	.4072
6	.5814	.4784
7	.8273	.5440
8	1.1111	.6046
9	1.4301	.6605
10	1.7819	.7119
11	2.1635	.7590
12	2.5721	.8018
13	3.0048	.8405
14	3.4589	.8750
15	3.9312	.9054
16	4.4191	.9317
17	4.9195	.9540
18	5.4297	.9723
19	5.9470	.9867
20	6.4687	.9972
21	6.9923	1.0039
22	7.5152	1.0067
23	8.0352	1.0058
24	8.5499	1.0012
25	9.0574	.9929
26	9.5556	.9810
27	10.0426	.9656
28	10.5168	.9464
29	10.9766	.9239
30	11.4206	.8976
31	11.8474	.8678
32	12.2559	.8340
33	12.6451	.7967
34	13.0139	.7545
35	13.3616	.7084
36	13.6871	.6555
37	13.9898	.5967
38	14.2672	.5246
39	14.3868	.4787
40	14.5011	.4208
41	14.6214	.3766
42	14.7403	.3289
43	14.8610	.2859
44	14.9817	.2430
45	15.1033	.2027
46	15.2253	.1636
47	15.3480	.1266
48	15.4712	.0914
49	15.5951	.0587
50	15.7195	.0282
51	15.8450	.0023

Table 8

Case 7

CD4, LAM., $Re_L = 10^6$

I	X/R	r/R
1	0.0000	0.0000
2	.0072	.1568
3	.0383	.3106
4	.0939	.4573
5	.1724	.5932
6	.2716	.7148
7	.3883	.8191
8	.5209	.9037
9	.6649	.9663
10	.8167	1.0057
11	.9730	1.0201
12	1.1695	1.0230
13	1.4086	1.0253
14	1.6887	1.0280
15	2.0072	1.0314
16	2.3695	1.0326
17	2.7443	1.0343
18	3.1534	1.0355
19	3.5822	1.0361
20	4.0242	1.0356
21	4.4729	1.0344
22	4.9217	1.0317
23	5.3637	1.0282
24	5.7924	1.0230
25	6.2015	1.0171
26	6.5852	1.0091
27	6.9384	1.0009
28	7.2567	.9398
29	7.5366	.9791
30	7.7752	.9543
31	7.9713	.9503
32	8.1676	.9156
33	8.1515	.8484
34	8.2493	.7956
35	8.3460	.7357
36	8.4460	.6775
37	8.5468	.6189
38	8.6487	.5613
39	8.7513	.5050
40	8.8543	.4504
41	8.9575	.3976
42	9.0609	.3469
43	9.1643	.2985
44	9.2676	.2523
45	9.3710	.2084
46	9.4742	.1669
47	9.5774	.1278
48	9.6806	.0912
49	9.7838	.0574
50	9.8872	.0268
51	9.9912	.0010

Table 9

Case 8

R4, LAM., $Re_L = 10^6$

I	X/R	r/R
1	0.0000	0.0000
2	.0051	.1222
3	.0267	.2070
4	.0647	.2814
5	.1186	.3494
6	.1880	.4125
7	.2725	.4717
8	.3718	.5273
9	.4854	.5798
10	.6129	.6292
11	.7538	.6756
12	.9075	.7191
13	1.0734	.7598
14	1.2509	.7975
15	1.4392	.8324
16	1.6376	.8643
17	1.8453	.8932
18	2.0616	.9191
19	2.2854	.9420
20	2.5160	.9617
21	2.7524	.9783
22	2.9937	.9918
23	3.2389	1.0020
24	3.4872	1.0089
25	3.7373	1.0125
26	3.9885	1.0128
27	4.2397	1.0096
28	4.4896	1.0037
29	4.7379	.9929
30	4.9829	.9791
31	5.2240	.9618
32	5.4601	.9406
33	5.6901	.9157
34	5.9133	.8866
35	6.1285	.8535
36	6.3347	.8154
37	6.5311	.7728
38	6.7162	.7235
39	6.8887	.6674
40	7.0150	.6137
41	7.1225	.5285
42	7.2442	.4652
43	7.3639	.3980
44	7.4967	.3363
45	7.6103	.2773
46	7.7357	.2215
47	7.8523	.1688
48	7.9934	.1197
49	8.1203	.0744
50	8.2510	.0339
51	8.3842	.0009

Table 10

Case 9

HEMI., TURB., $Re_L = 10^6$

I	X/R	r/R
1	0.0000	0.0000
2	.0005	.0528
3	.0040	.1255
4	.0115	.1879
5	.0230	.2497
6	.0386	.3105
7	.0582	.3702
8	.0817	.4285
9	.1091	.4850
10	.1401	.5397
11	.1746	.5922
12	.2124	.6423
13	.2535	.6899
14	.2975	.7347
15	.3443	.7766
16	.3938	.8153
17	.4456	.8508
18	.4996	.8829
19	.5556	.9113
20	.6133	.9362
21	.6726	.9570
22	.7330	.9742
23	.7946	.9868
24	.8567	.9959
25	.9194	.9996
26	.9823	1.0002
27	1.0299	.9833
28	1.0585	.9430
29	1.1161	.9070
30	1.1628	.8649
31	1.2103	.8205
32	1.2576	.7736
33	1.3048	.7252
34	1.3517	.6757
35	1.3984	.6256
36	1.4447	.5755
37	1.4909	.5258
38	1.5371	.4767
39	1.5834	.4286
40	1.6298	.3819
41	1.6766	.3366
42	1.7239	.2931
43	1.7716	.2515
44	1.8200	.2120
45	1.8693	.1748
46	1.9187	.1400
47	1.9691	.1076
48	2.0200	.0776
49	2.0712	.0497
50	2.1228	.0240
51	2.1746	.0004

UNCLASSIFIED

SECURITY CLASSIFICATION OF THIS PAGE (When Data Entered)

REPORT DOCUMENTATION PAGE

READ INSTRUCTIONS BEFORE COMPLETING FORM

1. REPORT NUMBER: MDC G7823	2. GOVT ACCESSION NO.
3. RECIPIENT'S CATALOG NUMBER	
4. TITLE (and Subtitle): OPTIMUM TAIL FAIRINGS FOR BODIES OF REVOLUTION.	5. TYPE OF REPORT & PERIOD COVERED: Final rept.
6. PERFORMING ORG. REPORT NUMBER: MDC-G7823	
7. AUTHOR(s): A. M. O. Smith, T. R. Stokes, Jr., R. S. Lee	8. CONTRACT OR GRANT NUMBER(s): N00014-77-C-0672
9. PERFORMING ORGANIZATION NAME AND ADDRESS: McDonnell Douglas Astronautics Company, 5301 Bolsa Avenue, Huntington Beach, California 92647	10. PROGRAM ELEMENT, PROJECT, TASK AREA & WORK UNIT NUMBERS
11. CONTROLLING OFFICE NAME AND ADDRESS: Office of Naval Research, 800 N. Quincy Street, Arlington, Virginia 22217	12. REPORT DATE: Mar[illegible]979
	13. NUMBER OF PAGES: 50
14. MONITORING AGENCY NAME & ADDRESS(if different from Controlling Office): Ship Performance Department, David W. Taylor Research and Development Center, Bethesda, Maryland 20084, Code 1505	15. SECURITY CLASS. (of this report): Unclassified
	15a. DECLASSIFICATION/DOWNGRADING SCHEDULE

16. DISTRIBUTION STATEMENT (of this Report)

Approved for public release; distribution unlimited

17. DISTRIBUTION STATEMENT (of the abstract entered in Block 20, if different from Report)

18. SUPPLEMENTARY NOTES

19. KEY WORDS (Continue on reverse side if necessary and identify by block number)

Fluid mechanics	Transition	Body of revolution
Subsonic	Separated flow	Tail fairing
Boundary layer	Skin friction	

20. ABSTRACT (Continue on reverse side if necessary and identify by block number)

This report describes a computerized method that will design tails for bodies of revolution that satisfy the Stratford criterion for zero wall shear. Stratford's original two-dimensional solution is extended to axisymmetric flow in order to implement the procedure. The method involves simultaneous solution of the extended Stratford equation and the necessary boundary conditions through the use of an inverse potential flow program. Tails designed with this procedure can be categorized as follows: 1) The

DD FORM 1 JAN 73 1473 EDITION OF 1 NOV 65 IS OBSOLETE

UNCLASSIFIED

SECURITY CLASSIFICATION OF THIS PAGE (When Data Entered)

389 310

entire tail is at incipient separation (no skin friction); 2) The pressure recovery is the most rapid possible; 3) The resultant tail is the shortest possible. The final result is a unique geometry for given freestream conditions and boundary layer transition point. By unique, it is meant that any deviation from the "ideal" geometry will either cause extensive separation or the tail must become longer and, hence, contribute to skin friction and reduced volumetric efficiency.

The computer program can operate in one of two modes: 1) The forebody geometry can be maintained (except for a very small region near the tail juncture) with only the tail shape determined by the method; 2) The forebody velocity distribution can be maintained up to the point of the pressure recovery. The forebody geometry will then be altered for some distance upstream of the tail juncture. A number of solutions are presented for both of the above modes. Although the report emphasis is on bodies of revolution, the concept is also applicable to two-dimensional flows.